8-2007

ANALYZING RELATIONSHIPS BETWEEN LIGHTNING AND RAIN IN ORDER TO IMPROVE ESTIMATION ACCURACY OF RAIN

Justin Lapp
Clemson University, jlapp@clemson.edu

ANALYZING RELATIONSHIPS BETWEEN LIGHTNING AND RAIN IN ORDER TO IMPROVE ESTIMATION ACCURACY OF RAIN

A Thesis
Presented to
the Graduate School of
Clemson University

In Partial Fulfillment
of the Requirements for the Degree
Master of Science
Mechanical Engineering

---

by
Justin L. Lapp
August 2007

Accepted by:
Dr. John R. Saylor, Committee Chair
Dr. Richard S. Miller
Dr. Carlton W. Ulbrich

ABSTRACT

The remote estimation of rainfall rate R is essential for the aviation industry, agriculture, and flood warning. Radar, the current means of R estimation, is not available in much of the world. In addition, this measurement involves a level of inaccuracy. Using lightning to detect rain is a relatively inexpensive alternative to radar systems and can be done from existing satellites. Previous research has revealed correlations between lightning and rain, suggesting either that it is possible to estimate R using lightning, or that it is possible to use it to correct for a portion of the radar inaccuracies. These correlations are not only between the amount of lightning and the amount of rain, but also between other parameters, including statistics describing raindrop size.

Rain, lightning, and radar data were collected in Central Florida over a two month period in the summer of 2005. Rain data, including raindrop size statistics, were collected from a single point using a disdrometer. Lightning data were collected using the Los Alamos Sferic Array. Radar data were obtained from the WSR-88D radar network.

Rain rate R and the raindrop size statistics were compared to lightning statistics to determine which rain/lightning parameter pairs were most correlated. The degree of correlation between rain and lightning parameters was evaluated using the correlation coefficient r. Different lightning types (Cloud-to-Ground, Intra-Cloud, Narrow-Bipolar-Event, Total) were considered, and various circular areas were used for lightning collection to optimize the strength of the correlations.

Four models using lightning and/or radar for the estimation of R were developed and then compared for accuracy. The first model is based on the relationship between R and the radar reflectivity factor Z, as is the current practice. Two models using only lightning for the estimation of R were evaluated, and a final model used both radar and lightning data to estimate R. The performance of each model was evaluated using the RMS error.

The correlations between rain and lightning parameters were generally weak ($r < 0.5$), although some pairs clearly produced stronger correlations than others. Results show that the strongest correlations are between lightning density (strokes/km^2/hr) and Λ, a parameter of the raindrop size distribution. This correlation was strongest for Intra-Cloud (IC) lightning measured on a 75 km diameter.

Results from the R estimation models indicate that the use of lightning alone is a valid alternative to the use of radar for the conditions studied ($R > 0.1$ mm/hr, lightning present). The method combining radar and lightning parameters produces more accurate estimations of R than either type alone. Based on these results, lightning data can be used in addition to radar to provide greater accuracy to publicly available rain estimates, and it can be used to provide rain estimation capability to new locations, including greater flood warning ability.

ACKNOWLEDGMENTS

I would like to thank the following people for their tremendous assistance to my research and the completion of my thesis: Dr. Carl Ulbrich for his assistance in collecting and understanding the rain data in this research, including the use of the disdrometer; Dr. Herman Senter for his instruction and consultation about the statistical methods which made this research possible. Dr. Richard Miller for his advice and instruction, specifically on Fortran programming; Ms. Barbara Ramirez for her assistance with writing and revising this thesis, and Dr. T. E. Lavezzi-Light, Jeremiah Harlin, and Kyle Wines, all of LANL, for their consultation on all aspects of LASA and other lightning data.

I would like to thank my fellow graduate students in Dr. Saylor's lab group for their friendship and assistance, and Meg Iannacone for her love and support.

Funding for my research, and LASA lightning detection data were provided by Los Alamos National Laboratories (LANL). Facilities for collection of rain data were provided by Dr. Daniel L. Colvin of the University of Florida, with on-site assistance provided by James A. Boyer, also of the University of Florida. WSR-88D radar data were obtained from the National Climatic Data Center. I would like to thank all of these individuals and organizations for easy access to the data that made my work possible.

Finally, I want to thank my graduate advisor Dr. John Saylor, for all his guidance and advice, which has helped me maintain quality in all of the research, writing, and communication I have done throughout my work at Clemson.

TABLE OF CONTENTS

Page

TITLE PAGE . . . . . **i**

ABSTRACT . . . . . **iii**

ACKNOWLEDGEMENTS . . . . . **v**

LIST OF TABLES . . . . . **viii**

LIST OF FIGURES . . . . . **x**

NOMENCLATURE . . . . . **xii**

CHAPTER

1 INTRODUCTION **1**
- 1.1 Radar 1
- 1.2 Drop-Size-Distribution (DSD) 3
- 1.3 Lightning background 5
- 1.4 Early direct relationships between lightning and rain 7
- 1.5 Studies involving lightning parameters other than n 9
- 1.6 Studies involving the DSD and lightning 11

2 OBJECTIVES **13**

3 METHODS **15**
- 3.1 Rain Data 15
- 3.2 Lightning data 18
- 3.3 Radar data 22
- 3.4 Calculating lightning parameters 24
- 3.5 Computing correlations between lightning and rain parameters . . 25
- 3.6 Calculating r and the p-value 26
- 3.7 Estimating R from Z: radar only method 27

Table of Contents (Continued)

Page

3.8 Estimating R from a single lightning measurement: lightning only method 30
3.9 Estimating R from two lightning measurements using the DSD: lightning DSD method 30
3.10 Estimating R from Z and lightning with a purely statistical approach: radar/lightning method 31

4 RESULTS 33
4.1 Bulk lightning statistics 33
4.2 Correlation of lightning and R 33
4.3 Correlations of DSD parameters 41
4.4 Radar only method 47
4.5 Lightning only method 49
4.6 Lightning DSD method 50
4.7 Radar/lightning method 54
4.8 Comparison of estimation methods 54

5 DISCUSSION 57
5.1 Relative strength of lightning and rain parameters 57
5.2 Performance of lightning types 61
5.3 Adjusted lightning density 62
5.4 Comparison of R estimation methods 63
5.5 Rain estimation using a combined radar/lightning model 64

6 CONCLUSION 67

APPENDIX: DETAILED CORRELATION RESULTS 69

REFERENCES 81

LIST OF TABLES

Table		Page
1	Experimental DSD bin centers s_i and bin widths w_i recorded by Joss-Waldvogel disdrometer.	17
2	Sample DSD data file.	17
3	Sample of LASA data.	20
4	Bulk statistics of lightning collected for this study.	34
5	Correlation results of R and n_s, showing values of r with p-values shown in parentheses.	36
6	Best relationships for each pair of rain and lightning parameters.	47
7	Summary of the errors produced by the three rain estimation methods studied for $D = 25$ km.	55
8	Summary of the errors produced by the two rain estimation methods studied for $D = 75$ km.	55
A-1	Relationships between R and n_s.	69
A-2	Relationships between R and $n_{s,a}$.	70
A-3	Relationships between R and q.	71
A-4	Relationships between R and F.	72
A-5	Relationships between Λ and n_s.	73
A-6	Relationships between Λ and $n_{s,a}$.	74
A-7	Relationships between Λ and q.	75

List of Tables (Continued)

Table Page

A-8 Relationships between Λ and F. 76

A-9 Relationships between N_0 and n_s. 77

A-10 Relationships between N_0 and $n_{s,a}$. 78

A-11 Relationships between N_0 and q. 79

A-12 Relationships between N_0 and F. 80

LIST OF FIGURES

Figure Page

1 Joss-Waldvogel type momentum disdrometer shown with tipping-bucket rain gage, installed for data collection. 16

2 Experimentally measured DSD shown as the solid line, with the exponential fit DSD shown as the dashed line. 18

3 Locations of LASA stations in the Florida array. 19

4 Sample radar image. 23

5 Results location table. 26

6 Plots of R versus n_s of the four lightning types. 35

7 Plot of r for each D for the relationship of R and n_s. 39

8 Plot of r for each D for the relationship of R and $n_{s,a}$. 39

9 Plot of r for each D for the relationship of R and q. 40

10 Plot of r for each D for the relationship of R and F. 40

11 Plot of Λ versus total lightning density n_s. 41

12 Plot of N_0 versus total lightning density n_s. 42

13 Plot of r for each D for the relationship of Λ and n_s. 42

14 Plot of r for each D for the relationship of N_0 and n_s. 43

15 Plot of r for each D for the relationship of Λ and $n_{s,a}$. 44

List of Figures (Continued)

Figure Page

16 Plot of r for each D for the relationship of N_0 and $n_{s,a}$. 45

17 Plot of r for each D for the relationship of Λ and q. 45

18 Plot of r for each D for the relationship of Λ and F. 46

19 Experimental R-Z relationship developed for KMLB WSR-88D station at the disdrometer location. 49

20 Plot of R and F for CG lightning on the 25 km domain, with best fit exponential relationship. 50

21 Plot of Λ and IC $n_{s,a}$ on the 75 km domain, the strongest correlation involving Λ. 51

22 Plot of N_0 and CG $n_{s,a}$ on the 75 km domain, the strongest correlation involving N_0 on the 75 km domain. 52

23 Evaluation of the lightning DSD method. 53

24 Statistical method of estimating R using a multiple regression with predictors Z and F for CG lightning on the 25 km domain. . . . 55

NOMENCLATURE

Rain Modeling

DSD	Drop-size-distribution
N_0	Intercept parameter of the DSD
$N(s)$	Value of the DSD at s
R	Rain rate
R_a	Measured rain rate
R_e	Estimated rain rate
R_t	Rainfall total
s	Raindrop size
$v(s)$	Terminal vertical velocity of drop size s
w	Width of experimental DSD drop size bin
Z	Radar reflectivity factor
Λ	Slope parameter of the DSD
μ	Parameter used in 3-parameter DSD

Lightning Modeling

CD	Cloud discharge
CG	Cloud-to-ground lightning
IC	Intra-cloud lightning
NBE	Narrow-bipolar-event lightning
D	Analysis domain size
F	Fraction of total lightning which is a specific type
q	Lightning percent positive

n	Lightning flash count
n_s	Lightning stroke density
$n_{s,a}$	Lightning stroke density adjusted for area of radar reflectivity

Statistical Analysis

RMS	Root-mean-square error
RMS_{log}	Root-mean-square error calculated in log space
p-value	Confidence of non-zero fit indicator
r	Correlation coefficient

Equipment and Other Abbreviations

LANL	Los Alamos National Laboratories
LASA	Los Alamos Sferic Array
NLDN	National Lightning Detection Network
RF	Radio Frequency
WSR-88D	Weather Surveillance Radar (19)88 Doppler

1 INTRODUCTION

Accurate estimation of rainfall rate R assists with agriculture and aviation, contributes to the understanding of weather systems, and is essential for flood forecasting. Several methods can be used for this estimation. Rainfall amounts (not rates) can be measured simply and effectively by using volumetric ground-based rain gages. To obtain R in real time, weighing and tipping-bucket rain gages can be used. All of these types of gages are able to take measurements only at a single point in space, requiring multiple installations to obtain any spatial information. To address this limitation, precipitation radars have become a common tool for estimating R, as they possess the ability to take measurements in real-time over large areas (460 km diameter for WSR-88D[3]) with a single ground installation. However, estimating R from these radars involves a level of inaccuracy. Most precipitation radars record a single parameter, the reflectivity factor Z. Since a universal relationship between Z and rainfall rate R has not been found[6], meteorologists typically rely on empirical relationships, which typically have errors of 50%[9]

1.1 Radar

Radar is important to R estimation for its ability to take real-time measurements over large geographic areas. The measurand obtained by a radar that is useful for lightning estimation is reflectivity Z, which is the amount of radio-frequency (RF) radiation reflected back to the radar station by the atmosphere, usually measured in decibels. Because forms of water, either liquid or solid, reflect much more RF radiation than clear air, radar has excellent performance for determining the location of precipitation. The difficulty in using radar for rain estimation is that

there is no universal relationship between R and Z. Rather, Z is related to the drop size distribution $N(s)$ (DSD) as shown by Doviak and Zrnic[6]:

$$Z = \int_0^\infty N(s) s^6 ds \tag{1}$$

where s is the drop diameter. The DSD can be used to find R by integrating over all drop sizes, using the following equation:

$$R = \frac{\pi}{6} \int_0^\infty N(s) s^3 v(s) ds \tag{2}$$

where $v(s)$ is the terminal vertical component of the velocity of drop diameter s. Therefore if Z could be used to find $N(s)$, then Eq. (2) could be used to find R. This is not possible because a description of $N(s)$ requires more than one parameter, and therefore can not be obtained by a single measurement of Z. Instead, empirical relationships between R and Z are used.

R and Z are often distributed evenly on log axes, and previous results have revealed that power law relationships fit well[9, 16]. These relationships vary significantly with geographic location, season, or rain type[16, 9, 32]. Doviak and Zrnic[6] present a multitude of power law relationships between R and Z found by many authors, including commonly used relationships such as:

$$R = 200 Z^{1.6} \tag{3}$$

found by Marshall *et al.*[16] and used for stratiform rain, and:

$$R = 300 Z^{1.5} \tag{4}$$

found by Joss and Waldvogel[9].

Improving the accuracy of radar over a standard R-Z relationship requires more

than one measured parameter. Dual-polarization radars measure two reflectivities simultaneously, one vertical and one horizontal. As water drops become larger, their shape becomes less spherical and more oblate. Oblate drops will cause a different horizontal and vertical reflectivity to be measured, so the ratio of these two reflectivities can be used as an additional parameter to fully determine $N(s)$[6]. Dual-polarization radars are not commonly used, and are expensive to install. A method using Z and a lightning parameter to find $N(s)$, on the other hand, is more convenient and cost effective. The WSR-88D network of radar installations provides coverage of Z measurements for nearly all of the continental United States, as does the National Lightning Detection Network (NLDN) for lightning measurements. Similar networks operate in other parts of the world such as Europe, so a method which uses a combination of lightning and single-polarization radar information is currently feasible, and is one focus of the research performed here. Any method of this type would rely on a relationship between lightning and some parameter of the DSD, which will be discussed in the following section.

1.2 Drop-Size-Distribution (DSD)

The drop-size-distribution (DSD) is a tool used to describe rain activity in more detail than is provided by R. The DSD specifies, for each drop size, the likelihood of that sized drop falling. It is similar to a probability density function, however it is not normalized to integrate to unity. The true DSD is function without a specific shape, so it would take an indefinite number of parameters to mathematically describe. It is typically approximated well by the form the DSD developed by Marshall and Palmer[15], known as the exponential DSD:

$$N(s) = N_0 e^{-\Lambda s} \tag{5}$$

where $N(s)$ is the density of the DSD, s the raindrop size, and N_0 and Λ are free parameters which vary based on the specific case to which the exponential DSD is applied. The exponential DSD will be used in the current research.

When expressed graphically on a log-log plot, the exponential DSD appears as a line with an intercept specified by N_0, and a slope following -Λ. This form of the DSD has been shown to fit well in most cases[6]. The primary advantage of the DSD over simply using R is that the two variables contain more information about rain than the single value R. The DSD is useful for R estimation because two measurements can be used to estimate Λ and N_0, then these estimates can be plugged into Eqs. (5) and (2) to find R, thus estimating R using information from two measurements instead of one.

It was noted that dual-polarization radar is capable of measuring two parameters simultaneously, enough to fully describe the exponential DSD without an additional measurement, such as a lightning parameter. If dual-polarization radar is used, lightning could still be used for improved accuracy in R estimation through use of a DSD form which has more than two variables. For example, a more accurate form of the DSD, using three parameters instead of two, has been suggested by Ulbrich[29], with μ being the additional parameter.

$$N(s) = N_0 s^{\mu} e^{-\Lambda s} \tag{6}$$

If two of the three parameters in Eq. (6) are fit by horizontal and vertical reflectivities from a dual-polarization radar, then the third can still be fit to a lightning parameter. A method such as this could benefit from both the capabilities of dual-polarization radar and the correlations between lightning and rain presented in this work.

1.3 Lightning background

Research on lightning became wide-spread in the later part of the 19th century, when photography became popular, a fact recognized by Uman[30] in his analysis of the past 100 years of lightning investigation. As he explains, lightning has been observed in thunderstorms, or convective rain clouds, stratiform rain clouds, clouds producing no rain at all, and perhaps even clear air. The vast majority of lightning occurs during thunderstorms.

Lightning can be divided into two general types, cloud-to-ground (CG) and cloud discharges (CD). The former is defined as any lightning discharge connecting to the earth, while the latter does not. CG lightning has been investigated much more than CD lightning, as it causes the vast majority of property damage, power outages, injuries, and deaths[5], despite comprising less than half of lightning discharges occurring within thunderstorms[30]. Uman[30] lists cloud discharges as including the following subtypes: intra-cloud (IC), which occur within a single cloud, cloud-to-cloud, which have initiation and termination points in separate clouds, and cloud-to-air discharges, which initiate within a cloud but terminate in clear air. Because IC discharges are much more common than other types, and experimental data, such as those used in the current research, cannot differentiate between these types[30], all cloud discharges in this research will be classified as IC. This practice is typical for the type of data used in this research.

Also included in IC lightning is a more recently discovered type known as narrow-bipolar-event (NBE). NBE's, which emit very intense radio-frequency radiation, have a short duration ($<$20 μs)[28] are optically weak[13] and are spatially compact[25]. Because of low optical emission, NBE lightning went undiscovered prior to the use of electric field change sensors for lightning detection[12]. A portion of the radiation from an NBE is sufficiently high in

frequency to pass into space[8], unlike radiation from most lightning, which is dispersed or blocked by the ionosphere. This means that space-based detection of NBE's is more efficient than for other lightning types. On earth, NBE lightning accounts for about 1% of all lightning[25], but can be as much as 40% of lightning detected from space[13]. A relationship between rain and NBE lightning could lead to improvements in space-based precipitation estimation. NBE lightning has not been previously related to rain to the author's knowledge.

As Uman[30] explains, an overall lightning discharge, either CG or IC, typically occurs on a path several kilometers in length and lasts for a duration between one half and one second. The entire event, known as a lightning flash, includes a leader, or an initial connection between the two end points of the lightning discharge, and one or more return strokes, which move the majority of the electric charge. As many as 20 or more return strokes may occur in one lightning flash, but globally, a mean of 3.5 strokes occur per flash.

Each lightning stroke may be either positive or negative, depending on whether it moves positive or negative charge between its origination and termination points. Negative CG lightning is more common than positive CG lightning, because clouds are usually negatively charged at the bottom, near the earth, and positively changed near the top. Negative CG lightning usually originates from the bottom of the cloud, transferring tens of coulombs of negative charge to ground and producing electrical currents having an average of 30 kA per return stroke. Positive CG lightning usually originates from the top of the cloud, often from the positively charged "anvil dome", which is sheared off the top of the thunder-head by high altitude winds. Positive lightning typically travels further and is more intense, lowering hundreds of coulombs of charge to ground, and commonly achieving currents over 100 kA. IC lightning, both positive and negative, transfers tens of

coulombs of charge like negative CG lightning, but produces lower currents on return strokes because more current flows continuously through its channel, transferring charge without the need for intense return strokes.

1.4 Early direct relationships between lightning and rain

A direct relationship between rain and lightning is sought because it could provide an alternative method to radar for R estimation. Classical lightning-rain studies correlate directly the amount of lightning and the amount of rainfall. One of the first studies, conducted in 1965 in Arizona by Battan[1], found that the relationship between amount of rain that fell in a set period R_t and the number of CG lightning flashes observed n was modeled best by the power law relationship:

$$n = 3.3R_t^{1.3} \tag{7}$$

Battan[1] also grouped days into "heavy rain" and "light rain", finding that about 0.03 mm of rain fell per lightning flash in either category.

In similar research, Kinzer[10] examined squall line storms in June in Oklahoma, determining that approximately 50% less rain was produced per lightning flash than in Battan's[1] study. Kinzer's[10] study included only a single storm system, occurring over a five-hour period, and did not disprove Battan's[1] results. Kinzer's[10] work did initiate a discussion of the apparent variation in lightning-rain relationships based on location and/or storm.

Instead of a power law relationship like Battan[1] or Kinzer[10], Piepgrass *et al.*[20] found that a linear correlation between n and R fit the data well, with little scatter when considering only an individual thunderstorm. For the two storms examined, the relationships:

$$n = 3 + 13R \tag{8}$$

and:

$$n = 21 + 26R \tag{9}$$

were developed. As can be seen, the second storm, fit with Eq. (9), exhibits more than twice as much lightning per unit of rainfall. This study was one of the first to use lightning data collected by electric field change measurements, as opposed to visual counting of lightning as was used in Refs. 1 and 10.

Zhou *et al.*[33] found that a logarithmic fit of the form:

$$R = 1.69 \ln n - 0.27 \tag{10}$$

worked best. Although power law fits are the most common for relating lightning and rain, Piepgrass *et al.*[20] and Zhou *et al.*[33] have shown that other forms can work as well. These studies, however, considered limited sets of thunderstorm data, two days in the case of Zhou *et al.*[33] and individual storms in the case of Piepgrass *et al.*[20].

Often, lightning-rain correlations are presented in the form of the average weight of rain falling per lightning flash in order to permit a simple comparison of lightning-rain relationships in different geographic locations and regardless of fit type. These values, in kg/flash, are known as "rain yields." For example, Petersen and Rutledge[19] examined how location affects lightning-rain relationships, finding that rain yields ranged within the United States from 5.7×10^7 kg/flash in the arid Southwest to 2.5×10^8 kg/flash in the north-central areas. This value for the Southwest agrees with the rain yield found in Battan's[1] study, which ranged from 3-6$\times10^7$ kg/flash. In Florida, Piepgrass and Krider[20] found smaller values of 1.8×10^7 and 2.2×10^7 kg/flash for the two storms considered, while Lopez *et al.*[14], who also studied Florida storms, found that rain yields varied from 10^7 to 10^9 kg/flash using radar-derived R. All of these studies considered only cloud-to-ground

lightning.

Rain yield values vary in other parts of the world as well. Near Paris, for example, Soula and Chauzy[26] measured between 5×10^7 and 10^8 kg/flash, while in Australia, Williams *et al.*[31] obtained a higher value of 5×10^9 kg/flash, and found that rain yields for individual storms ranged between 9×10^7 and 10^{10} kg/flash. According to Petersen and Rutledge's[19] study of tropical regions, rain yields vary from 3.4×10^8 to 10^{10} kg/flash.

These ratios between the bulk lightning and rain amounts are useful to our physical understanding of thunderstorms, and the variation shows that a universal relationship between the amount of lightning and the amount of rain is unlikely to exist. Strong correlations can be found for limited sets of data, but a more complex method appears to be necessary for reliable estimation of R.

1.5 Studies involving lightning parameters other than n

In addition to correlating rainfall to lightning counts, alternative lightning characteristics have been used. The percent of measured positive polarity is an example of one of these alternative lightning characteristics that have been studied for possible correlations to rain. This parameter is commonly referred to as p in other literature. To avoid confusion with p-value, which will be introduced in Section 3, the symbol q will be used in this study for the measured percent of lightning strokes that are of positive polarity. As previously noted, lightning can either transfer positive or negative charge to ground[30]. The waveforms of these types of lightning, as measured with electric field change sensors, are inverted from each other, and are defined as positive or negative lightning based on the initial slope of the waveform. The recorded waveforms depend on the sensor array hardware and processing software, so the definition of a positive or negative stroke

depends on the array used to collect lightning data. Strokes designated as positive by one array may be designated negative by another array. Therefore, although most arrays in North America operate on the same classification system, values of q in this work could be comparable to (100-q)% from some other studies, though none are known to the author at this time. This should be understood when comparing studies which include q derived from different arrays.

Murty *et al.*[18] noted that q was higher during times of low precipitation, but did not add q to any mathematical relationships. Sheridan *et al.*[24] showed that adding q to relationships that already include n improved the coefficient of determination r^2 significantly, reducing the unexplained scatter by between 16% and 31%. Using radar estimates, Seity *et al.*[22] computed the volume of rainfall per flash RV in units of 10^3 m^3/flash and correlated it to q for CG flashes. A linear relationship was found:

$$RV = 6.87q + 8.73 \tag{11}$$

Soula and Chauzy[26] performed a similar analysis, and found the linear relationship:

$$RV = 6.18q + 38.15 \tag{12}$$

Seity *et al.*[22] used 10 days of non-frontal storm data and Soula and Chauzy[26] used four days of non-stratiform storm data.

Soula and Chauzy[26] also examined the effect of lightning types on the lightning-rain relationship. Using lightning data that included intra-cloud (IC) lightning as well as CG, they noted that days with a high ratio of CG lightning flashes to total lightning flashes also had lower values of rainfall volume per CG flash, calculated using radar estimates. A parameter based on the ratio of the lightning types was not used in curve fits, and this study was limited to four days of thunderstorms near Paris.

Although CG lightning compromises a minority fraction of overall detectable lightning (about 25% in the current data set), each of the aforementioned studies searched for a relationship between rainfall and lightning primarily by considering CG lightning. Soula and Chauzy[26] made brief mention of IC lightning, but, as noted, did not find analytical relationships. The main reason for this focus on CG lightning is that measurements of other lightning types have not been available until recently. Early lightning detection networks focused on detecting lightning that causes property damage *viz.* CG lightning. Hence many of the early lightning detection networks were designed to ignore other types of lightning[4]. This notwithstanding, some research has suggested that other lightning types and quantifiers other than n may be useful when relating rainfall to lightning (e.g. Refs. [18, 24, 26]). Following these studies, q, and ratios of lightning types were examined in the current research.

1.6 Studies involving the DSD and lightning

Recently, DSD parameters were compared to lightning data as an alternative to comparing lightning directly to R. Saylor *et al.*[21] suggested that a better approach might be to correlate lightning to statistical characteristics of rain (i.e. parameters of the DSD), and then use these sub-correlations to obtain a relationship between lightning and rain. Saylor *et al.*[21] correlated lightning stroke density n_s for CG lightning, obtained from the National Lightning Detection Network (NLDN), to N_0 and Λ of the exponential DSD shown in Eq. (5). It was found that n_s was correlated more strongly to Λ than to N_0 or R. However, prediction of R using correlations of (N_0, Λ) to n_s resulted in prediction errors that were similar to those from a direct relationship between n_s and R. In the Saylor *et al.*[21] study, both N_0 and Λ were estimated from the same n_s measurement, which is a possible reason for

the similarity in prediction errors. The errors for the method involving the DSD may be smaller if different parameters (n_s, q) and/or different lightning types (CG, IC, NBE) are used to estimate N_0 and Λ.

The overarching goal of this study is to improve the accuracy of real-time remote rainfall estimation, through the use of lightning information. This may be possible through a method which relies only on lightning data, or through a combination of lightning and radar data. This study first investigates how several lightning parameters are related to R and parameters of the exponential DSD, to determine which parameters may be best used in a model for the estimation of R. Then several models for estimating R are evaluated against the current method using radar.

2 OBJECTIVES

The first objective of this work is to identify which rain parameters and lightning parameters are most strongly correlated. These results will further the understanding of lightning and its relation to the physical processes in thunderstorms, but will primarily be used to select parameters which can be used for accurate estimation of R. Lightning parameters can be calculated using four lightning types (CG, IC, NBE, Total), so an objective is to determine which lightning type can be used to obtain maximum correlation strength. In addition, this research seeks to determine the area on which to measure lightning parameters for strongest correlations. Because NBE lightning is efficiently detected from space, this research will specifically seek to identify relationships using NBE lightning which may be used for accurate rain estimation.

A main objective of this work is to determine if radar information, lightning information, or a combination of the two most accurately estimates R. Where radars are available, the method with the strongest accuracy may use only radar, only lightning, or a combination of the two. This research will determine which proposed method (lightning only or lightning-radar combined) provides the greatest accuracy compared to the current radar only method. For use in areas without available radar, this research will seek a method using only lightning. A method of this type could be implemented through use of only an existing satellite, or by a ground lightning detection network, which would be inexpensive compared to a radar network. In investigating a lightning only method, this research will also determine if estimating R through relationships between DSD parameters and lightning is more accurate than directly estimating R from a single lightning parameter.

3 METHODS

3.1 Rain data

In this work, three main data types were collected: rain data, including the DSD, lightning data, and radar data. Rain data were collected using a Joss-Waldvogel type momentum disdrometer (Disdromet RD-69 with attached ADA-90 analyzer) placed near Citra, Florida at a site provided by the University of Florida. A tipping-bucket type rain gage was also installed at the disdrometer location for comparison to the disdrometer data. Both instruments are shown in Fig. 1, with a 12 inch rule for scale. These instruments collected data continuously from 17 May 2005 to 11 July 2005. Lightning and radar data were obtained for this time period, and herein, all analyses use the complete data set encompassing these dates, without excluding specific storm types, weather conditions, or other variables.

When rain drops hit the circular foam cone of the disdrometer, shown in Fig. 1, a piezoelectric element senses the momentum transferred from the drop to the cone. This momentum is then equated to a drop size, and a count is added to one of the twenty size bins, shown in Table 1. At the end of each one minute interval, the counts in these bins are recorded in a text file, and reset. Part of a sample text file is shown in Table 2.

The DSD drop histograms were totaled over one hour time intervals, then converted to a probability density function in units of number of drops per volume of air in m^3 per unit size interval in mm. The DSD was then fit with the exponential, shown in Eq. (5), and (Λ, N_0) were found by least-squares curve fitting. This process is shown in Fig. 2, with a sample DSD, collected for this research, fit by the DSD formulation shown. For each time interval, an exponential

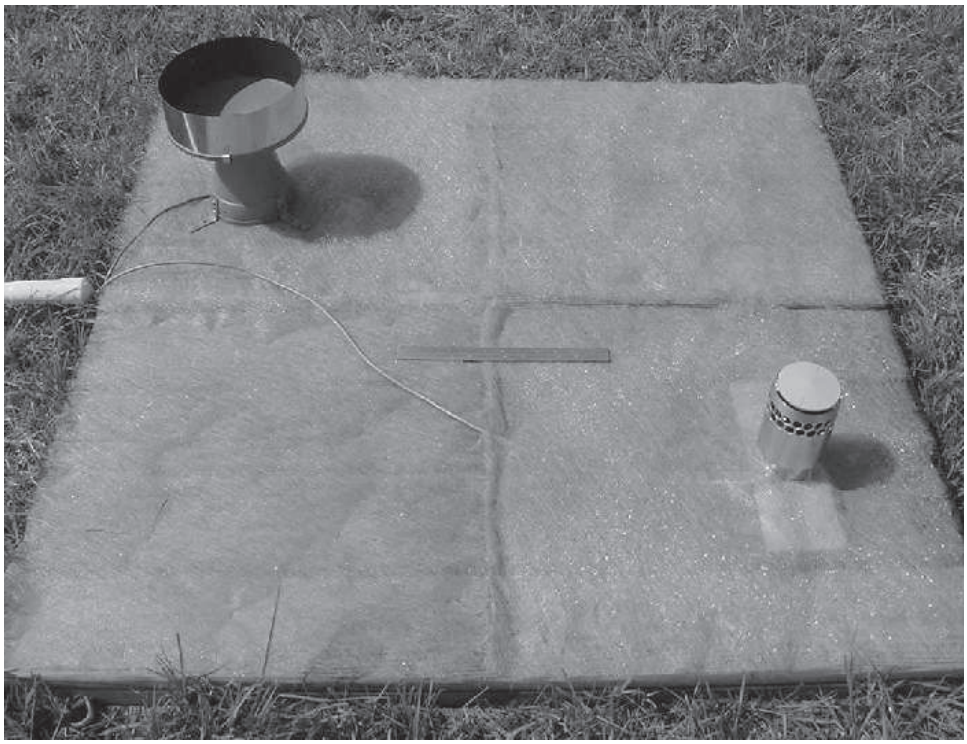

Figure 1: Joss-Waldvogel type momentum disdrometer shown with tipping-bucket rain gage, installed for data collection. Fiberglass material was attached to the installation platform around the instruments to reduce spatter from drops that did not hit the instruments

Table 1: Experimental DSD bin centers s_i and bin widths w_i recorded by Joss-Waldvogel disdrometer.

Bin	s_i (mm)	w_i (mm)
1	0.35	0.1
2	0.45	0.1
3	0.55	0.1
4	0.65	0.1
5	0.75	0.1
6	0.90	0.2
7	1.10	0.2
8	1.30	0.2
9	1.50	0.2
10	1.70	02
11	1.95	0.3
12	2.25	0.3
13	2.55	0.3
14	2.85	0.3
15	3.15	0.3
16	3.50	0.4
17	3.90	0.4
18	4.30	0.4
19	4.75	0.5
20	5.25	0.5

Table 2: Sample DSD data file. Data occurred on 29 June 2005, between 15:49 and 15:54, as indicated by the time indicator in the first column. Other columns are the number of drops in each size bin, increasing in size from left to right.

	s_i (mm)												
Time	0.35	0.45	0.55	0.65	0.75	0.90	1.10	1.30	1.50	1.70	1.95	2.25	2.55
1549	1	1											
1550	1	1	0	1	1	5	1	0	0	1			
1551	1	4	4	4	5	23	42	25	22	17	18	11	6
1552	5	5	11	16	28	81	115	108	27	30	24	11	1
1553	2	12	26	27	39	80	135	100	21	12	5		
1554	5	16	27	34	42	94	114	26	15	3	1		

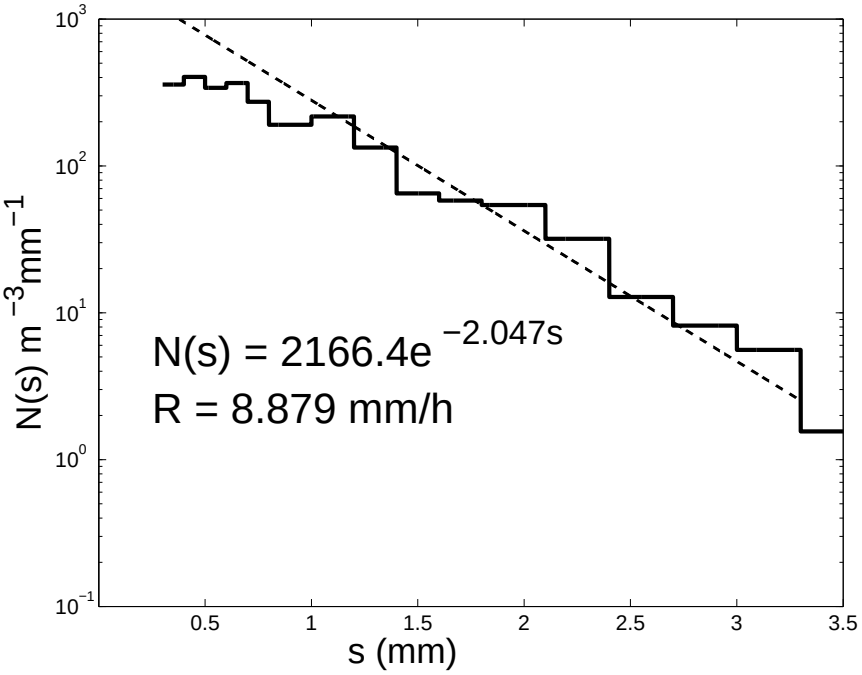

Figure 2: Experimentally measured DSD shown as the solid line, with the exponential fit DSD shown as the dashed line. The equation for this fit is shown, with Λ equaling 2.047, and N_0 equaling 2166.4. This DSD was collected for the period from 2000-2100 UTC on 21 May 2005, and R was 8.879 mm/hr.

fit was found, and R was calculated through Eq. (2). The resulting (R, Λ, N_0) were recorded as the rain data products to be correlated to lightning. When specified by the fitting procedure, Λ has units of mm^{-1} and N_0 has units of $\text{m}^{-3}\text{mm}^{-1}$.

3.2 Lightning data

Lightning data were collected by Los Alamos National Laboratories (LANL) using the Los Alamos Sferic Array (LASA)[23], and shared for this work. The LASA consists of eight electric field change sensor stations located in Florida, and other stations located in New Mexico and Nebraska. Although all stations operate as a single array, lightning for this study was primarily sensed by the Florida portion of the array. Stations outside of Florida only contribute to lightning detection if that

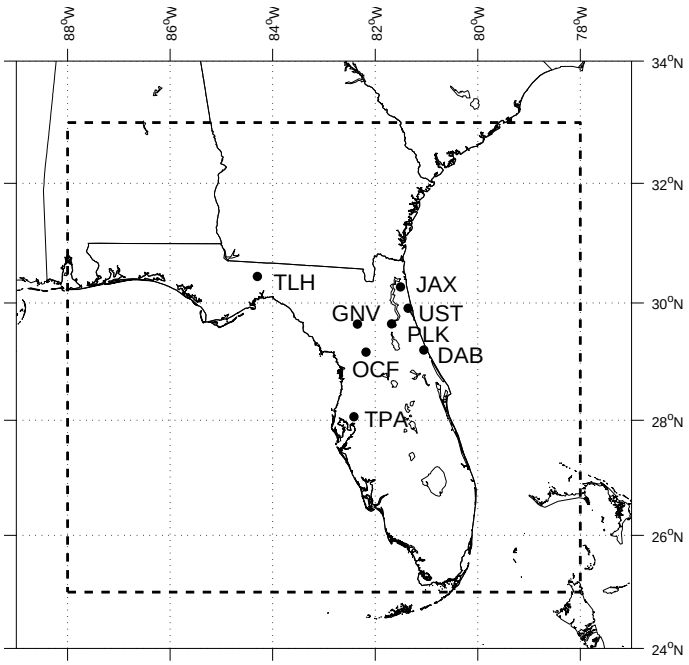

Figure 3: Locations of LASA stations in the Florida array.

lightning was sensed by less than four of the Florida stations, but by at least one station in other regions. This situation is highly unlikely for data in this study, which are located completely within the Florida array, but is necessary for the detection of lightning in locations such as the Gulf of Mexico or the Rocky Mountains. The Florida station locations are shown in Fig. 3.

LASA stations record radio-frequency (RF) waveforms from sensed lightning, which are sent to LANL for processing. Time-of-arrival techniques are used to determine a precise latitude/longitude location for each lightning event. Unlike many other lightning detection networks, such as the NLDN, waveforms are processed to identify RF signals reflected by the ionosphere, permitting a measurement of the altitude of each lightning event. This altitude is used to differentiate IC lightning from CG lightning. NBE lightning is identified by the speed of the waveform rise and fall. The amplitude of the waveform is used to

Table 3: Sample of LASA data. Columns are, from left to right, date, hour, minute, second, latitude, longitude, lightning type, peak current.

20050517	18	24	45.518507	28.8872	-82.4600	CG	-12.0
20050517	18	24	45.518528	28.8879	-82.4615	CG	-12.0
20050517	18	24	45.518544	28.8825	-82.4312	CG	-11.9
20050517	18	24	45.555554	28.8866	-82.4603	CG	-7.6
20050517	18	24	45.829721	28.9164	-82.4553	IC	-2.4
20050517	18	24	50.838919	29.1210	-82.5399	IC	2.4
20050517	18	24	50.841262	29.1228	-82.5399	NB	2.9
20050517	18	24	50.856719	29.1194	-82.5384	IC	7.7
20050517	18	24	50.856738	29.1212	-82.5365	IC	7.7

compute a peak electrical current for each lightning event, as well as to determine the polarity.

LASA data were received from LANL as text files which included a time stamp, latitude/longitude location, identification of type, and peak current for each event. A sample of a portion of one data file received from LANL is shown in Table 3. Each line of the file contains information about one lightning event, which typically corresponds to a lightning stroke. Often in these data, multiple events are listed with nearly identical time and location, indicating that more than one event corresponds to the same lightning stroke. This is due to the array detecting the same lightning stroke several times, using multiple groups of sensors which co-locate the event at slightly different locations. Branched or stepped lightning can also cause multiple events to be detected from the same stroke. The data were processed to identify which events were part of a single stroke, and which strokes were part of a single flash. The data do not include indication of which events were part of one stroke, or which strokes combined to form flashes.

Lightning events were grouped into strokes, and strokes were grouped into flashes by a similar method. When an initial event was identified, subsequent events which were sufficiently close in both space and time were designated to be part of the first. For grouping events into strokes, subsequent events which followed within

1 ms, and occurred no more than 500 m from the first were considered to be the same stroke. The location, time, and polarity (positive or negative) of a stroke with multiple events were set to those of the first event. No differentiation was made between strokes that were composed of only one event and those composed of multiple events. When grouping strokes into a flash, strokes subsequent to the first must follow within 1 s, and occur no more than 1000 m from the first. The location and time of the flash were set to that of the first stroke, and the number of strokes contained within a flash is defined as the multiplicity and recorded for each flash. Any events/strokes which could be grouped into multiple strokes/flashes were grouped into the stroke/flash nearest in location.

Each event was identified within the data as either IC, CG, NBE, or unknown. At the stroke level, types other than unknown were kept separate, meaning that events of two different types could not be grouped in the same stroke. When combining strokes into flashes, however, CG and IC strokes could be grouped into the same flash. This choice was made by LANL because IC lightning occurs in the cloud above a CG flash, feeding more charge to the bottom of the cloud which can be transferred to ground by CG lightning[30]. Grouping these IC and CG strokes together in a flash is meant to treat this activity as a single lightning process. The first stroke of a CG flash did not necessarily have to be a CG stroke, so if any stroke in a grouping of IC and CG strokes was CG, then the entire flash was designated CG. A flash was designated as IC only if it was composed entirely of IC strokes. NBE strokes were not grouped into IC or CG flashes, nor were IC or CG strokes grouped into NBE flashes. This process reflects the theory that NBE lightning is caused by a separate process from other lightning. Strokes of an unknown type were grouped into any type of flash for which the time and location criteria were met.

These flash data were used to calculate several lightning parameters, which are

correlated to rain parameters, the main results of this work.

3.3 Radar data

Radar stations record Z at several elevations, or angles from the ground at which signals are sent. At each elevation, the station must rotate 360 degrees, because at any instant, a signal can only be sent along one vector radiating from the station. In typical precipitation-mode operation, WSR-88D stations measure Z at several elevations (the exact number varies with the mode that the radar is operating within, usually 12-14 for the data in this work), while making the rotation for each elevation in approximately 30 seconds[3]. A full set of elevations, known as a sweep, is collected about every six minutes. The lowest of these elevations, on which the signal is sent on a vector with an angle of 0.5 degrees above ground, is known as the base elevation[3]. Because it is low to the ground, it detects few clouds, so Z from this elevation is a good estimator for the location of precipitation and is used to estimate R[7].

WSR-88D (NEXRAD) radar data were obtained from the National Oceanic and Atmospheric Administration. These data include several parameters, one being Z. Data were obtained from the Melbourne, Florida WSR-88D station (KMLB). The Jacksonville, Florida (KJAX) station is slightly closer to the disdrometer location than KMLB, but data from KJAX were found to have several errors and periods of missing data. All radar data presented here were measured by the KMLB WSR-88D station. Fig. 4 shows a sample of one hour of averaged base Z.

Base Z was extracted from the data, and used for two purposes. First, it was used as a parameter to estimate rain. To do this, the average value of Z was found on a 5 km diameter centered on the disdrometer. This average Z was obtained for each sweep which started during the period of data collection. These values were

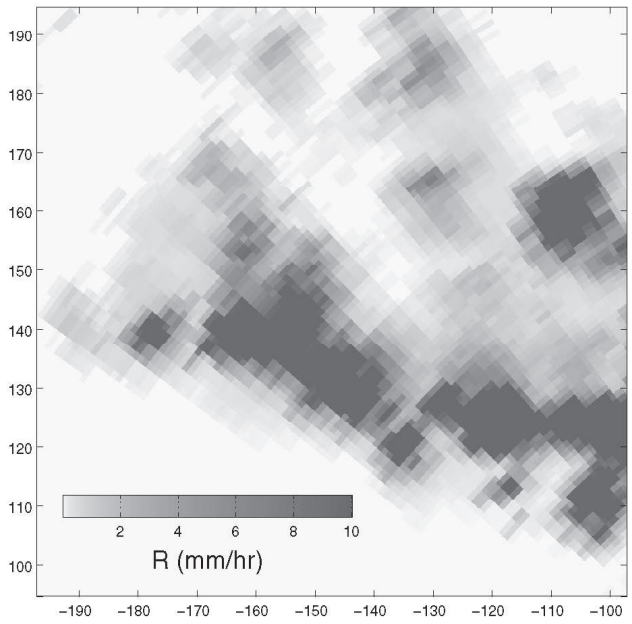

Figure 4: Sample radar image. The area shown in the image is centered on the disdrometer, and is 100 km on each side.

averaged over the time period to arrive at a single value of Z for that period. These data were used to estimate R using a power law relationship, following the same procedure used for estimating R from Z at most National Weather Service stations. This gives a standard of performance to compare against for the new methods examined in this work. These values of Z were also used in an experimental method where a multiple regression is used to estimate R, with Z and lightning parameters both used as estimators.

Additionally, Z was found for the entire analysis domain on which lightning parameters were computed, and used to correct stroke density values by allowing for lightning which is only occurring in the portion of the domain where the radar indicates rainfall. This is described further in the next sub-section.

3.4 Calculating lightning parameters

To examine the relationship between lightning and rain, and ultimately to build a model for estimating rain from lightning, various lightning parameters were calculated. For each of these, all lightning which occurred within a circular analysis domain during a specific time period was counted. The time period was one hour for all analyses done here. The analysis domains were all centered on the disdrometer location, so the lightning used would be all lightning within a specific radius from the rain measurement location. Nine analysis domains were examined, with diameters D of 10, 25, 50, 75, 200, 125, 150, 175, and 200 km.

Lightning stroke density n_s is the frequency of lightning strokes per area, and is calculated by counting the lightning which occurred within D during the time frame, and dividing by the area of the domain in km^2 and the time frame in hrs. This gives a value of n_s in strokes/km^2/hr. The calculation was done using the sum of all lightning, referred to as total lightning and for each individual lightning type (CG, IC, and NBE). This method assumes that lightning is occurring over the entire analysis domain, and that the density over this area is uniform. This is not likely the case, and results may be skewed by time periods where lightning occurred over only a small portion of the domain. This can be accounted for by using radar data.

WSR-88D (NEXRAD) base Z maps were extracted and averaged over the same one hour periods on which lightning and DSD data were totaled. The Z maps were converted to estimated R maps by use of a power law relationship developed for the current data set by fitting R (calculated from the DSD) to Z at the disdrometer location (measured by WSR-88D). The relationship developed is:

$$Z = 1084R^{1.12} \tag{13}$$

where R is in units of mm/hr and Z is in units of mm^6/m^3. The estimated R maps

were then thresholded by taking any area with an estimated R above 0.01 mm/hr (near the lowest R discernible by radar) as an area in which lightning is likely occurring. This area was totaled, and used in place of the total analysis domain area to compute lightning density. This new lightning density is referred to as the adjusted lightning stroke density $n_{s,a}$. Adjusting lightning density by radar information has not previously been performed in lightning-rain studies to the author's knowledge.

The percentage of strokes of positive polarity q, as measured by the LASA, is computed as the ratio of the number of positive lightning strokes to the total number of lightning strokes to obtain a value between zero and 100%.

The fraction of total lightning F for each type is computed by taking the number of strokes, both positive and negative, that occurred within the analysis domain for each of the three lightning types (CG, IC, NBE), and dividing by the total number of strokes of all types of lightning. This yields a value between zero and one, where one indicates that all lightning was of the type in question, and zero represents that there was lightning occurring, but none was of the type in question.

3.5 Computing correlations between lightning and rain parameters

For each of the nine analysis domains, R, Λ, and N_0 were compared to each lightning parameter (n_s, $n_{s,a}$, q, F) for each lightning type (total, CG, IC, NBE), and the correlation coefficient r and the p-value were computed for each case. These values comprise a large volume of information. The locations of the relevant plots or tables for each pair of parameters is shown graphically in Fig. 5. The relationships between rain parameters and n_s and $n_{s,a}$ were characterized by power law relationships. The relationships between rain parameters and the other two lightning parameters, q and F, were better characterized by exponential

		Rain Parameter		
		R	Λ	N_0
Lightning Parameter	n_s	Table 5 Figure 7	Figure 13	Figure 14
	$n_{s,a}$	Figure 8	Figure 15	Figure 16
	q	Figure 9	Figure 17	
	F	Figure 10	Figure 18	

Figure 5: Results location table. For each combination of one rain parameter, and one lightning parameter, the correlation coefficient r is computed for each lightning type and for each D. These values of r are presented in the Table or Figure listed.

relationships, of the form:

$$R = ae^{bq} \tag{14}$$

in the case of the relationship between R and q, with a and b found by least squares curve fitting.

This research focuses on conditions with both lightning and significant rain. Time periods are only considered if lightning is present, and R is 0.1 mm/hr or greater. The majority of these conditions are likely to occur during thunderstorms, or convective activity. Some stratiform rain conditions may exist within the data, but no processing was done to identify these data, or to remove them.

3.6 Calculating r and the p-value

The correlation coefficient r and the p-value were used to quantify the strength of each relationship. The value of r is a measure of how well the variation in one

variable corresponds to variation in the other and is defined as[17]:

$$r = \frac{\sum_{i=1}^{N}(X_i - \bar{X})(Y_i - \bar{Y})}{\left[\sum_{i=1}^{N}(X_i - \bar{X})^2 \cdot \sum_{i=1}^{N}(Y_i - \bar{Y})^2\right]^{1/2}} \tag{15}$$

where X and Y are the variables being correlated (which are assumed to be random and normally distributed), N is the number of data points, and the overbar denotes the mean of that variable.

The p-value gives a direct measure of relationship strength in percent confidence and permits comparison between relationships obtained using disparate numbers of data points (which is the case in this work). The p-value is the confidence that a relationship has no correlation, and can be thought of as one minus the confidence that there is a non-zero correlation. For example, a p-value of 0.1 indicates 90% confidence that there is a non-zero relationship. The following method is used to calculate the p-value. First, r is found by Eq. (15). This and the number of points N are used to compute the test statistic t^*:

$$t^* = \frac{r\sqrt{N-2}}{\sqrt{1-r^2}} \tag{16}$$

This t^* is then found in a table of the t-distribution with $N-2$ degrees of freedom, and the corresponding α or left tail percentile is found. The p-value is $1-\alpha$, or the right tail percentile. Only relationships with p-values below 0.05 ($> 95\%$ confidence) are considered significant herein, and those considered significant are ranked by r.

3.7 Estimating R from Z: radar only method

The value of Z, obtained in a 5 km diameter at the disdrometer location as described above, is plotted against R, obtained from the disdrometer to find the

best fit power law relationship between the two parameters. The relationship found in this work is not expected to resemble previously developed R-Z relationships because it will be only for periods where the rain rate was 0.1 mm/hr or greater, meaning little stratiform rain will likely be included, and the majority of the data will be from thunderstorm conditions. Due to calibration inaccuracies, and geographic differences, radar stations often use custom derived relationships between R and Z, so the relationship found in this work will have comparable accuracy to any number of relationships which are currently used, although specialized to situations where lightning methods would be applicable. This method may serve as a best case baseline of performance for a radar only method against which the lightning methods may be tested.

Herein, the quality of the remaining R estimation methods are compared to the quality of the radar only method. This will indicate if any of the new methods will result in increased accuracy over the standard method in an application. If any of the new methods display better quality of R estimation, quantified by parameters described below, then it is advisable to further explore these new methods in an application situation. If, however, all three new methods fail to predict R better than the radar only method, then it is advisable to continue estimation of R using only Z.

The best fit relationship between R and Z is found with least squares curve fitting, as are all curve fits in this work. The performance of each rain estimation method is evaluated by the root-mean-square (RMS) prediction error. This is found with the following equation:

$$\mathrm{RMS} = \sqrt{\frac{\sum_{i=1}^{N} \left(R_{e,i} - R_{a,i}\right)^2}{N}} \tag{17}$$

where $R_{e,i}$ is the estimated value of R, $R_{a,i}$ is the value of R measured by the disdrometer, and N is the number of points. The RMS will have a value in mm/hr, and a better performing fit will produce a lower RMS value. The RMS is often used to evaluate the quality of curve fits, but when points are not equally distributed on linear axes, individual points can greatly bias the RMS, because, for example, a point that is off by 50% at R=10 mm/hr will add much more to the RMS (10 times) than a point which is off by 50% at R=1 mm/hr, despite the inaccuracies for these two points having arguably the same importance.

An alternative is to find the RMS error in log space. This is logical because the curve fitting procedure is done in the log space, and because it would count the two points in the above example in a more balanced way. The equation for this procedure can be found by replacing R_e and R_a with the log of those values, and taking the exponential of the entire equation, to return the calculated value to units of mm/hr. The full equation is the following:

$$\mathrm{RMS}_{log} = \exp\sqrt{\frac{\sum_{i=1}^{N} \left(log(R_{e,i}) - log(R_{a,i})\right)^2}{N}} \tag{18}$$

The disadvantage of calculating this parameter in log space is the quantity will have less physical meaning than one in linear space. Although the units will remain in mm/hr, because the values have both the logarithm and exponential taken once each, the values of RMS_{log} do not correspond to a typical error in mm/hr as will the RMS. The meaning of the RMS_{log} will simply be that a method with a lower value will give reduced percentage error over all estimated values of R. Both the RMS and the RMS_{log} will be presented to show the quality of each rain estimation method.

3.8 Estimating R from a single lightning measurement: lightning only method

The method of estimating R from a single lightning measurement, which has been previously examined, is examined further in this work. Many previous studies of this relationship have been limited by using a single lightning type and/or a single parameter of lightning[1, 10, 21]. An objective described earlier in this study is to use a broad spectrum of lightning types (Total, CG, IC, NBE) and parameters (n_s,$n_{s,a}$,q,F) to find which lightning parameter was most correlated with R, and for which D that parameter should be calculated. The parameter found for this objective will be used to estimate R for the lightning only method.

As with the radar only method, the best fit relationship will be found, then this relationship will be used to calculate an estimated value of R at each data point. The quality of these predictions is evaluated by finding the RMS prediction error and the RMS_{log} prediction error. Methods with low values of RMS and RMS_{log} are more accurate.

3.9 Estimating R from two lightning measurements using the DSD: lightning DSD method

A slightly more complex, but promising method for estimating R from lightning was proposed by Saylor *et al.*[21]. The two parameters of the exponential DSD, Λ and N_0, were each estimated by lightning parameters. The exponential DSD was then integrated according to Eq. (2) to find R. This work tested the theory that even if lightning is not strongly related to the amount of rain R, it may be related to the type of rain, including drop size and number of drops. The previous work[21] did not find an improvement in accuracy by this method over a direct relationship between lightning and R, but in that analysis, both Λ and N_0 were estimated from

the same lightning parameter, possibly creating a dependent set of equations which would lead to poor accuracy.

In this work, a different lightning parameter is used to estimate each Λ and N_0. The only limitation is that both lightning parameters must be calculated for the same D, because they must include the same number of data points. The strongest relationship (as determined by r) with either Λ or N_0 for any D, is taken. Then for the other DSD parameter, the strongest relationship for the same D as the first relationship is found. These two relationships are used to find estimates of the DSD parameters, which are then plugged into the exponential DSD and integrated to find estimates of R, using Eqs. (2)-(5). These estimates of R are used to evaluate the accuracy of this lightning DSD method in the same way as previously discussed methods, by finding the RMS and RMS_{log}.

3.10 Estimating R from Z and lightning with a purely statistical approach: radar/lightning method

The final method of estimating R uses both radar and lightning information, and is simply a statistical model built with multiple regression. This model simulates the addition of lightning data to the currently used R-Z models, and could be easily implemented by assimilating data from the LASA or NLDN into radar systems in operation.

This radar/lightning method is produced by first deciding on a lightning parameter to add to the radar model. In this work, the lightning parameter most strongly correlated to R is used. Both this lightning parameter and Z are regressed on R. The one with a stronger r is then used to find initial estimates of R. The differences between these estimated values of R and actual R at each point are the residuals. The parameter which has the weaker correlation with R (Z or the

lightning parameter) is then regressed against the residuals. The two regression relationships are then added, arriving at a single relationship, in which a value of Z and of the lightning parameter can be used to estimate R.

This model is computed and evaluated like other methods, by calculating estimated values of R, then finding the RMS and RMS_{log} of these estimates. The accuracy of this method should be most closely compared to the radar only method. The radar/lightning method will likely provide some increase in accuracy over the radar only method, because the worst case scenario is that there is no relationship between the residuals and the parameter regressed on them. That situation would give this method the same accuracy as a single parameter method, such as the radar only method. If, however, there is a significant increase in accuracy, then this combination of radar and lightning data for the estimation of rain could provide an immediate increase in rain estimation capability from radar stations.

4 RESULTS

4.1 Bulk lightning statistics

Bulk statistics of lightning collected over the period of this study, from 17 May 2005 to 11 July 2005, are presented in Table 4 for D of 200, 100 and 25 km. These are presented to give a picture of the lightning composition used for correlation and model building analyses, and how they vary with D. It should be noted that individual IC strokes which occurred as part of a CG flash are counted towards the total number of CG strokes. This is a reason for the approximately equal totals of CG and IC strokes, while IC flashes comprise 60-70% of the total flashes, in agreement with previous results[23, 26]. These ratios remain nearly constant for the three analysis domains presented, implying that lightning composition is independent of D.

On average, CG flashes have approximately ten strokes (including some IC), while IC flashes have five, and NBE flashes have one. The data included a surprisingly high number of positive CG flashes, nearly as many as negative CG flashes. Previous research suggests that positive flashes make up less than 10% of CG lightning overall, and even less in summer storms [30]. The high percentage found in this data may be due to the classification system used with the LASA, or it may be an effect of the location (Central Florida) and/or season (summer).

4.2 Correlation of lightning and R

Relationships between rain rate R and lightning serve as a baseline of performance for relationships between DSD parameters and lightning. If DSD parameters are not correlated to lightning more strongly than R is to lightning, then rainfall estimation

Table 4: Bulk statistics of lightning collected for this study. For lightning types, percentages indicate the fraction of the total lightning which is of that type, i.e. CG comprises 29.1% of all lightning flashes. For positive lightning, percentages indicate the fraction of that type which is positive, i.e. 51.5% of CG flashes are positive.

$D = 200$ km		
Lightning Type	Flashes	Strokes
Total	168636	1143675
CG	49794 (29.5%)	551677 (48.2%)
+ CG	25641 (51.5%)	344609 (62.5%)
IC	105842 (62.8%)	576733 (50.4%)
+ IC	84938 (80.2%)	487878 (84.6%)
NBE	13000 (7.7%)	15265 (1.3%)
+ NBE	11005 (84.7%)	12992 (85.1%)
$D = 100$ km		
Lightning Type	Flashes	Strokes
Total	50843	343971
CG	14611 (28.7%)	161798 (47.0%)
+ CG	7504 (51.4%)	100692 (62.2%)
IC	32097 (63.1%)	177330 (51.6%)
+ IC	25607 (79.8%)	148132 (83.5%)
NBE	4135 (8.1%)	4843 (1.4%)
+ NBE	3547 (85.8%)	4170 (86.1%)
$D = 25$ km		
Lightning Type	Flashes	Strokes
Total	2706	16099
CG	698 (25.8%)	6818 (42.4%)
+ CG	323 (46.3%)	3755 (55.1%)
IC	1852 (68.4%)	9108 (56.6%)
+ IC	1522 (82.2%)	7773 (85.3%)
NBE	156 (5.8%)	173 (1.1%)
+ NBE	137 (87.8%)	151 (87.3%)

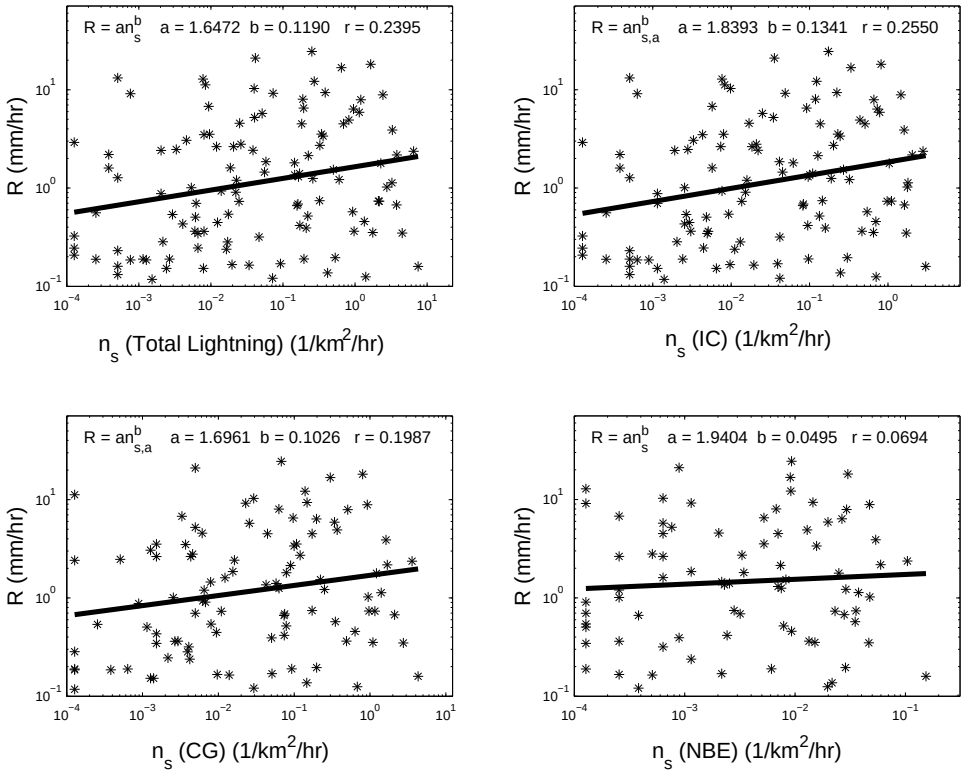

Figure 6: Plots of R versus n_s for the four lightning types. Clockwise from top-left: total, intra-cloud, cloud-to-ground, narrow-bipolar event. Solid lines indicate best fits to the indicated power law. Lightning densities were measured within a $D = 100$ km circle centered on the disdrometer location.

Table 5: Correlation results of R and n_s, showing values of r with p-values shown in parentheses.

D	Total Lightning	CG Lightning	IC Lightning	NBE Lightning
10 km	0.3323	0.1364	-0.1505	-0.4539
	(0.1179)	(0.6568)	(0.5924)	(0.1608)
25 km	0.1249	0.0260	0.1671	0.1683
	(0.2924)	(0.8653)	(0.1637)	(0.3195)
50 km	0.2663	0.0630	0.2925	0.0461
	(0.0071)	(0.5936)	(0.0030)	(0.7357)
75 km	0.2745	0.1841	0.2939	0.0322
	(0.0031)	(0.0842)	(0.0015)	(0.7896)
100 km	0.2395	0.1987	0.2550	0.0694
	(0.0096)	(0.0464)	(0.0057)	(0.5410)
125 km	0.2284	0.1357	0.2305	-0.0094
	(0.0121)	(0.1619)	(0.0117)	(0.9321)
150 km	0.2328	0.1564	0.2459	0.0549
	(0.0090)	(0.1045)	(0.0057)	(0.6053)
175 km	0.1973	0.1675	0.2082	0.0425
	(0.0224)	(0.1153)	(0.0195)	(0.5862)
200 km	0.1946	0.1352	0.2037	0.0184
	(0.0219)	(0.2135)	(0.0208)	(0.6739)

methods that involve DSD parameters would not produce more accurate results than a direct relationship between lightning and R. These results also identify which lightning parameters, lightning types, and D are used for rain estimation methods.

First, correlations were computed between R and lightning density n_s for CG, IC, NBE, and total lightning. Scatter plots of these relationships for the four lightning types on the $D = 100$ km domain are shown in Fig. 6. The plot shows a large amount of scatter for all types.

Table 5 presents a summary of the results presented in Fig. 6 for D=100 km, as well as results for the other domain sizes. This table is a more concise summary of correlation results, where just the r and p-value for the relationships between R and n_s are presented. Results from Table 5 are presented even more concisely in graphical form in Fig. 7 where r is plotted against D. The point on this plot having the largest absolute value of r reveals the best lightning type and D for that parameter pair. Only relationships with a p-value of 0.05 or lower are plotted.

Hereinafter, instead of presenting information in the form of scatter-plots like Fig. 6 or tables like Table 5, r for each combination of one lightning parameter and one rain parameter will be presented as in Fig. 7. A more complete summary of results, with r, p-value, and best fit curve for each relationship is given in Appendix A.

Figure 7 shows that the relationship between R and n_s is most strongly correlated for IC lightning on the 75 km domain, although the sensitivity of r to lightning type and D is small. IC and total lightning perform slightly better than CG lightning, while no significant correlation exists between R and n_s for NBE lightning, hence none of these data are plotted. High values of r can be seen in Table 5 on the 10 km domain, but due to very few data points being available for that D (15), the p-values for those relationships are too large for the relationships to be considered significant and they are not plotted. The relationship between R and n_s may be useful because of a significant correlation, at over 99% confidence in the case of IC or total lightning, but there is no lightning type or value of D for which R is correlated to n_s with $r > 0.3$, and a better relationship is desired.

Lightning density values were adjusted using radar, as described in Section 3, by replacing the area of the analysis domain with the thresholded area of high Z. Then, r was computed between R and this adjusted lightning density, $n_{s,a}$. Figure 8 shows the results of this analysis. The majority of relationships improve using $n_{s,a}$ (larger r and/or smaller p-value), but not significantly. The improvement is greater as D becomes larger. Accordingly, the decline in r on large domains is less apparent with $n_{s,a}$ than with n_s because, for many hours, although the larger domain added extra area, none of this area had lightning or radar reflectivity, but the radar adjustment threw out all of the extra area, and considered the hour in the same way as for the next smaller D. For n_s, the extra domain area changed the lightning density for these hours. The differences between n_s and $n_{s,a}$ relationships, however,

were generally minor, and the conclusions reached with the adjusted $n_{s,a}$ remain the same as for n_s.

Next, correlations were computed between R and measured percent positive q. These results are shown in Fig. 9. These relationships were fit with exponential functions of the form

$$R = ae^{bq} \tag{19}$$

as opposed to the power law functions used with n_s. Samples of relationships like Eq. (19) can be seen in Table 6. Several of these have an r exceeding 0.3, namely those for CG lightning for very large or very small D. All of the values of r in Fig. 9 are less than 0.4.

Correlations were computed between R and the fraction of total lightning F for each type, also with an exponential relationship of the form:

$$R = ae^{bF} \tag{20}$$

Results are shown in Fig. 10. There are only two points in this plot because the value of r was significant for only two cases: between R and F for CG lightning on the 25 and 50 km domains. On the 25 km domain, $r = 0.3878$, the strongest correlation with R for any lightning parameter, but it is not as strong as the r for several relationships between lightning parameters and Λ, which are presented below.

The presence of significant relationships between R and lightning parameters suggests some capability for directly estimating R from lightning. However, stronger correlations are desired.

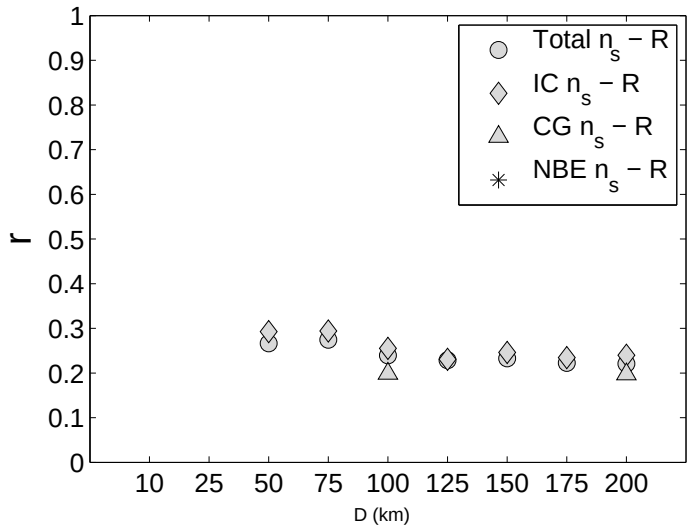

Figure 7: Plot of r for each D for the relationship of R and n_s. Only correlations with a p-value of 0.05 or lower are plotted. Note the strongest correlation is on a 75 km domain, and is for IC lightning.

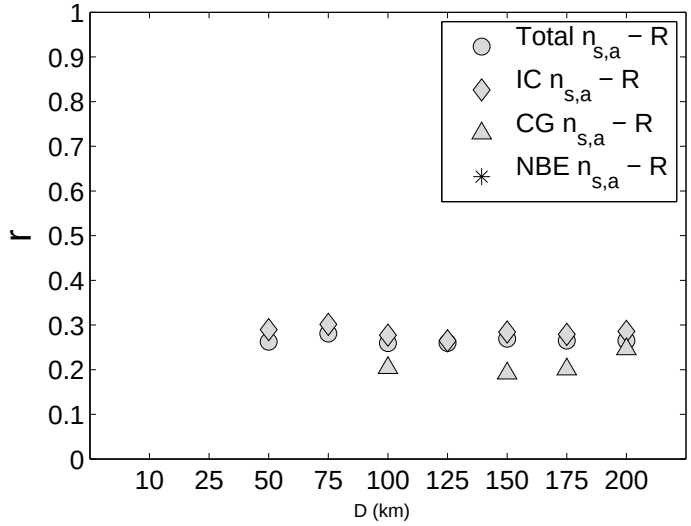

Figure 8: Plot of r for each D for the relationship of R and $n_{s,a}$. Only correlations with a p-value of 0.05 or lower are plotted. Note the strongest correlation is again on a 75 km domain, for IC lightning. Also note the reduced decline in r with D than for n_s due to adjustment by radar.

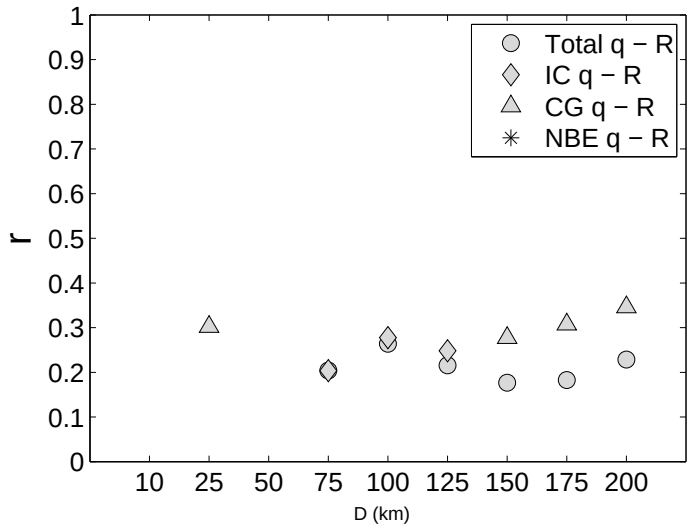

Figure 9: Plot of r for each D for the relationship of R and q. Only correlations with a p-value of 0.05 or lower are plotted. Note that here the strongest correlation is with CG lightning, and is on the 200 km domain.

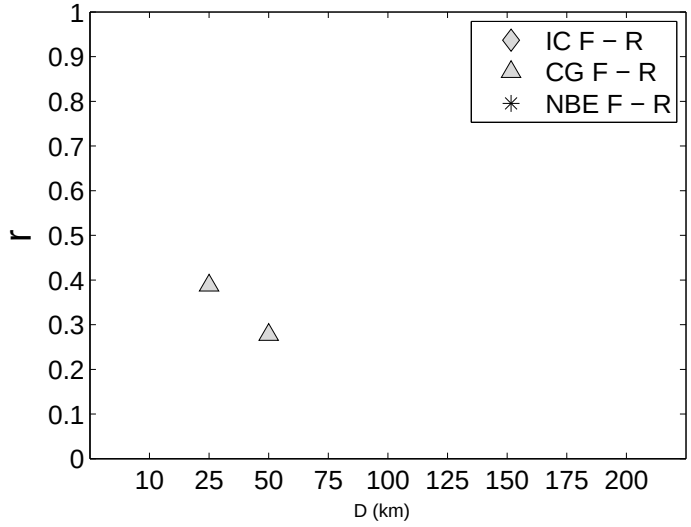

Figure 10: Plot of r for each D for the relationship of R and F. Only correlations with a p-value of 0.05 or lower are plotted. Note that here most correlations are not plotted because their respective p-values were not below 0.05.

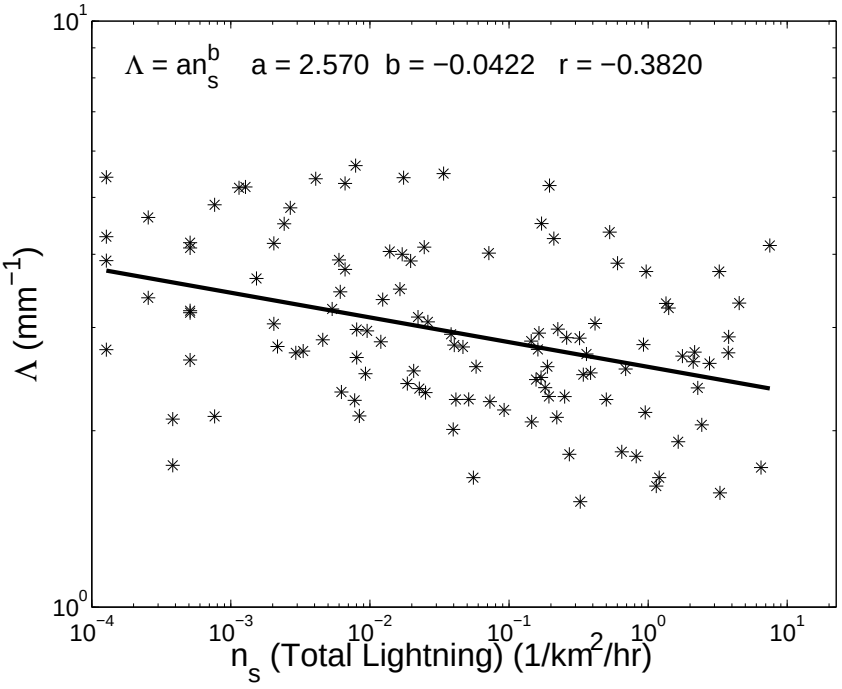

Figure 11: Plot of Λ versus total lightning density n_s. The solid line indicates best fit to the power law given on the plot. Lightning was measured on a 100 km diameter centered on the disdrometer.

4.3 Correlations of DSD parameters

Correlations were computed between the two exponential DSD parameters, Λ and N_0 and all lightning parameters that were examined in the above discussion: n_s, $n_{s,a}$, q, and F.

Figures 11 and 12 present example scatter plots of the relationship between Λ and n_s and between N_0 and n_s respectively, each for the 100 km domain. The plot of Λ versus n_s (Fig. 11) showed visibly less scatter than the plot of N_0 versus n_s (Fig. 12). Both showed less scatter than those for R (Fig. 6). This observation is supported by r, presented in Fig. 13 for Λ, and Fig. 14 for N_0. Relationships between DSD parameters and lightning have inverse trends, so values of r are negative. For these cases, plots, such as those in Figs. 13-14, have the y-axis inverted, plotting more negative values of r as higher points. The relationship

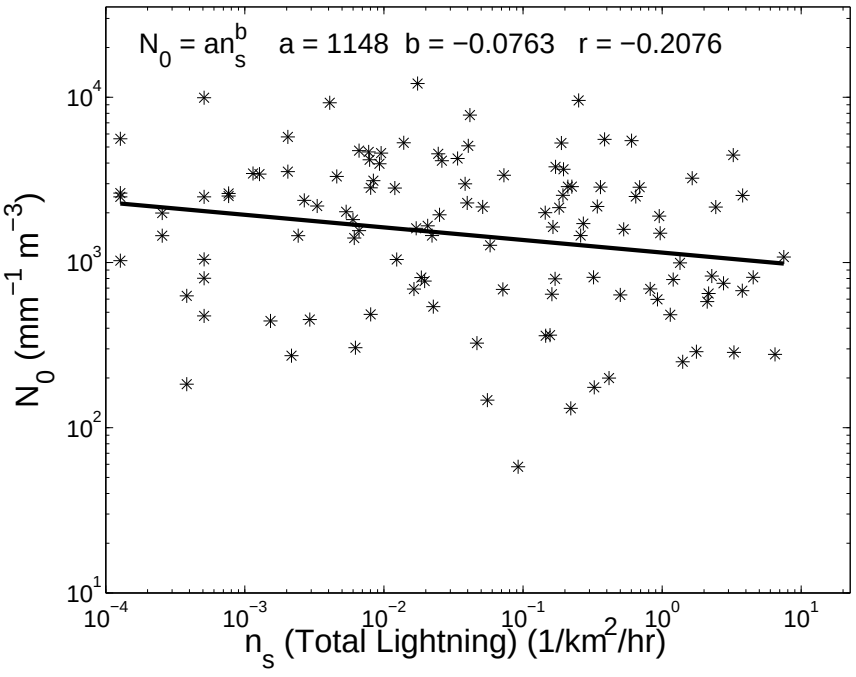

Figure 12: Plot of N_0 versus total lightning density n_s. The solid line indicates best fit to the power law given on the plot. Lightning was measured on a 100 km diameter centered on the disdrometer.

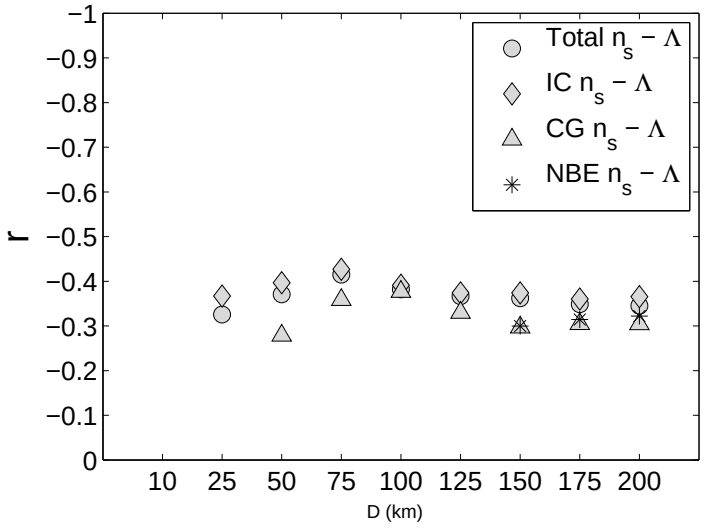

Figure 13: Plot of r for each D for the relationship of Λ and n_s. Only correlations with a p-value of 0.05 or lower are plotted. Note that values of r are stronger overall here than for R, and again the best correlation is on the 75 km domain for IC lightning.

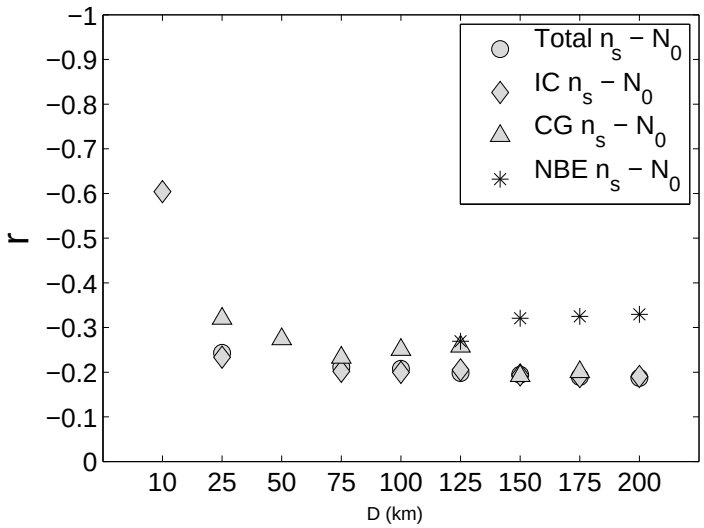

Figure 14: Plot of r for each D for the relationship of N_0 and n_s. Only correlations with a p-value of 0.05 or lower are plotted. Note that values of r are generally weaker than those between $\Lambda$and n_s. On small domains, CG n_s is most strongly correlated with N_0, but on large domains, NBE n_s is most strongly correlated.

between Λ and n_s is similar to the relationship between R and n_s, in the sense that r is strongest for IC followed by total lightning, and increases with D to 75 km, then declines as D continues to increase. However, the strongest r for Λ has an absolute value near 0.45, while that value for R is near 0.3.

The relationship between N_0 and n_s indicates that, for D of 100 km or smaller, CG lightning n_s is most correlated to N_0, and for D larger than 100 km, NBE lightning n_s is most correlated to N_0. Generally, relationships between N_0 and n_s were not as strong as those between Λ and n_s. An exception is the relationship between IC lightning n_s and N_0 on the 10 km domain (Fig. 14). This relationship displayed the strongest r found in this study, of -0.6042 and the p-value for this relationship was approximately 0.02, signifying a significant relationship. With only 15 data points, however, this relationship may be biased towards a single storm, or have some other irregularity that can not be accounted for by the p-value. This, and other relationships on the 10 km domain, do not include a sufficient number of data

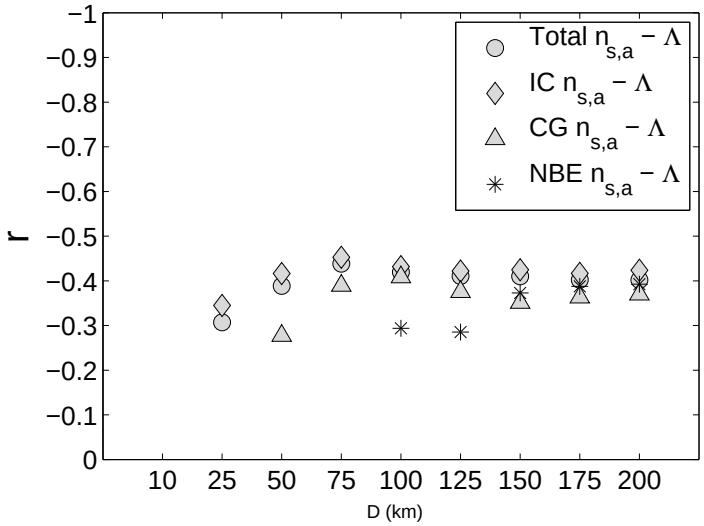

Figure 15: Plot of r for each D for the relationship of Λ and $n_{s,a}$. Only correlations with a p-value of 0.05 or lower are plotted. Note similarity with correlations of Λ and n_s, although values of r are stronger with $n_{s,a}$.

points to be considered representative of a long term trend, considering the variability of weather data from day to day or month to month. They will, however, be presented for completeness.

Correlations between DSD parameters and $n_{s,a}$ were computed, as was done for R. Results are shown in Fig. 15 for Λ and Fig. 16 for N_0. Relationships on domains of $D = 75$ km or larger all showed an increase in correlation strength from n_s, while on smaller domains, some improved, while others became worse. Λ was more correlated to $n_{s,a}$ than N_0 or R were correlated to $n_{s,a}$. This was the same result which was found with the non-adjusted n_s. The relationship between Λ and $n_{s,a}$ did not display as strong of a decline in strength with D as did the relationship between Λ and n_s. The correlations between Λ and $n_{s,a}$ are the strongest found in this study, with r nearing -0.5 for IC lightning on the 75 km domain.

Relationships between a DSD parameter and measured percent positive q were fit with an exponential function, as was done between R and q. The same form

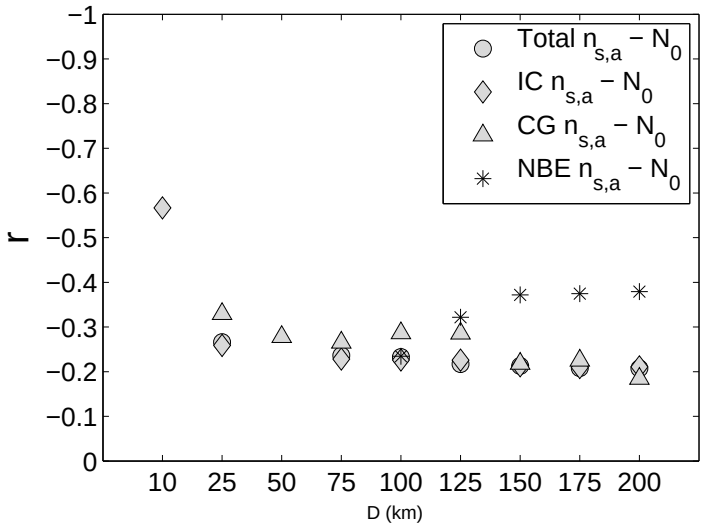

Figure 16: Plot of r for each D for the relationship of N_0 and $n_{s,a}$. Only correlations with a p-value of 0.05 or lower are plotted. Again, correlations are similar, but stronger for $n_{s,a}$ compared to n_s.

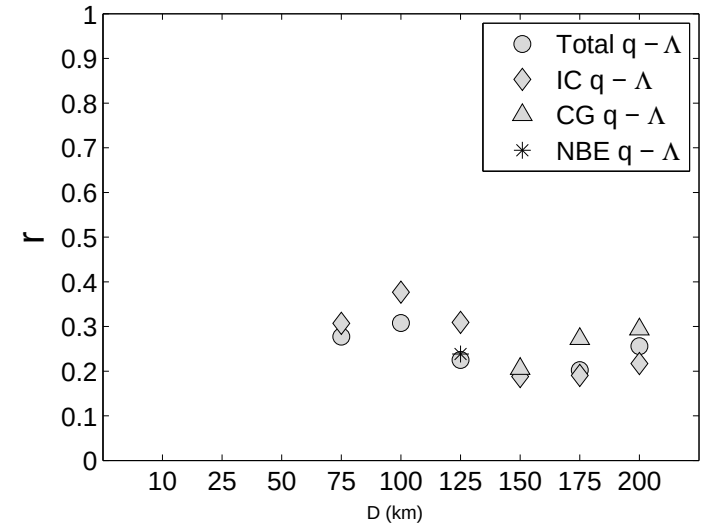

Figure 17: Plot of r for each D for the relationship of Λ and q. Only correlations with a p-value of 0.05 or lower are plotted. Note that the strongest correlation is for IC lightning on the 100 km domain.

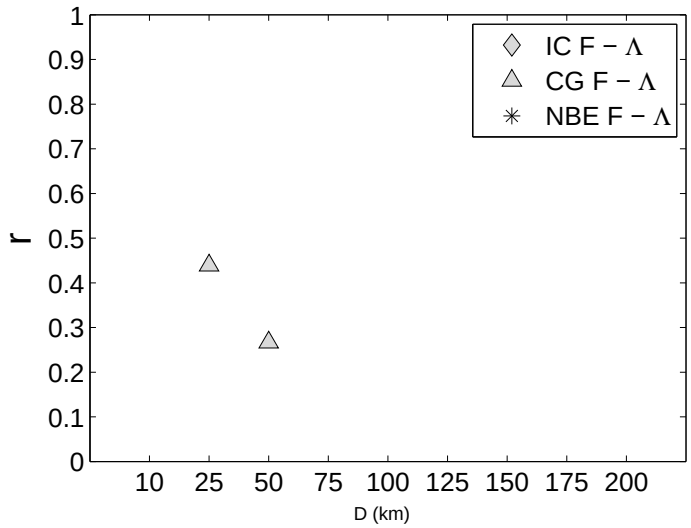

Figure 18: Plot of r for each D for the relationship of Λ and F. Only correlations with a p-value of 0.05 or lower are plotted. Note that only CG lightning F was significantly correlated to Λ, and only on the 25 and 50 km domain, although on the 25 km domain, the r of 0.4391 is strong compared to others in this study.

shown in Eq. (19) was used, except R was replaced with each of the DSD parameters. The results are shown in Fig. 17 for Λ. The relationship between Λ and q on the 100 km domain for IC lightning, where $r = 0.3766$ was the strongest involving q. For $D = 150$ km and larger, CG lightning q was most correlated to Λ, but not as strongly as IC lightning q was to Λ on the 75-125 km domains.

Values of r between N_0 and q are not plotted because no relationship produced a p-value below 0.05, so N_0 and q were not significantly correlated for any lightning type or on any analysis domain.

Finally, r was computed for the relationship between the DSD parameters and the fraction of total lightning F for each lightning type using an exponential fit similar to Eq. (20). Results are shown in Fig. 18 for Λ, which reveal a significant correlation only for CG lightning on the 25 and 50 km domains. On the 25 km domain, where $r = 0.4391$, the relationship is stronger than many found in this study, indicating that these parameters are strongly correlated, but only in a small

Table 6: Best relationships for each pair of rain and lightning parameters. One relationship is presented for each parameter pair, that for the lightning type and D that produced the best r. Relationships are sorted by r.

Rain Parameter	Lightning Parameter	Lightning Type	D	r	p-value	Relationship
Λ	$n_{s,a}$	IC	75 km	-0.4527	0.0000	$\Lambda = 2.45 n_{s,a}^{-0.0555}$
Λ	F	CG	25 km	0.4391	0.0025	$\Lambda = 2.05 e^{0.6394F}$
Λ	n_s	IC	75 km	-0.4269	0.0000	$\Lambda = 2.43 n_{s,a}^{-0.0506}$
R	F	CG	25 km	-0.3878	0.0085	$R = 4.09 e^{-2.3734F}$
N_0	$n_{s,a}$	NBE	200 km	-0.3792	0.0002	$N_0 = 511.9 n_{s,a}^{-0.1907}$
Λ	q	IC	100 km	-0.3766	0.0000	$\Lambda = 4.70 e^{-0.6034q}$
R	q	CG	200 km	-0.3459	0.0002	$R = 0.370 e^{2.0801q}$
N_0	n_s	NBE	200 km	-0.3294	0.0011	$N_0 = 516.3 n_s^{-0.1633}$
R	$n_{s,a}$	IC	75 km	0.3013	0.0011	$R = 1.96 n_{s,a}^{0.1654}$
R	n_s	IC	75 km	0.2939	0.0015	$R = 2.03 n_s^{0.1579}$

spatial area. No plot of the relationship between F and N_0 are shown because only one relationship was significant, that for IC lightning on the 75 km domain, where $r = 0.1844$.

A summary of the correlations between individual rain and lightning parameters is shown in Table 6. For each rain/lightning parameter pair, the lightning type and D which produced the strongest correlation are listed, along with r, the p-value, and the best fit relationship found. If a parameter pair did not produce any significant correlations, then it is not listed.

4.4 Radar only method

Base radar Z was averaged on a 5 km diameter, centered on the disdrometer, then averaged again over one hour periods. These values of Z were then compared to R obtained from the disdrometer. A power law curve was fit to the data, which can be seen in Fig. 19. The best fit relationship is specific to the radar station used, in this

case the Melbourne, FL WSR-88D station (KMLB), and the disdrometer location. In addition, as with analyses including lightning, only periods where $R > 0.1$ mm/hr were used. This results in a relationship resembling that for strong convective activity, with a larger leading coefficient, and a near-linear slope. Compare the relationship derived in this work:

$$R = 1143.9Z^{1.171} \tag{21}$$

to a commonly used R-Z relationship, developed by Joss and Waldvogel[9]:

$$R = 300Z^{1.5} \tag{22}$$

The RMS prediction error, defined in Eq. (17) will be used to evaluate the R estimation capability of the R-Z relationship developed in this work. The two R estimation methods using lightning, presented later, use data sets from different values of D, specifically 25 km for the lightning only method, and 75 km for the lightning DSD method. Because the data set for the larger D includes additional hours with lightning, these two methods will be evaluated by a different set of data points. Accurate comparisons can only be done between methods that use the same data points, because of outside conditions like temperature or storm type. To permit comparison between lightning methods and the radar only method, the radar only method will be developed twice using the same data points which are used in the two lightning methods. The radar only method using the same data points as the lightning only method will be referred to as the 25 km radar method, while the 75 km radar method will use the same data points as the DSD lightning method.

For the 25 km radar method, the RMS error equals 5.56 mm/hr. These data, as well as the best fit relationship, are presented in Fig. 19. Estimation methods will also be evaluated by the RMS_{log} prediction error, to account for the uneven

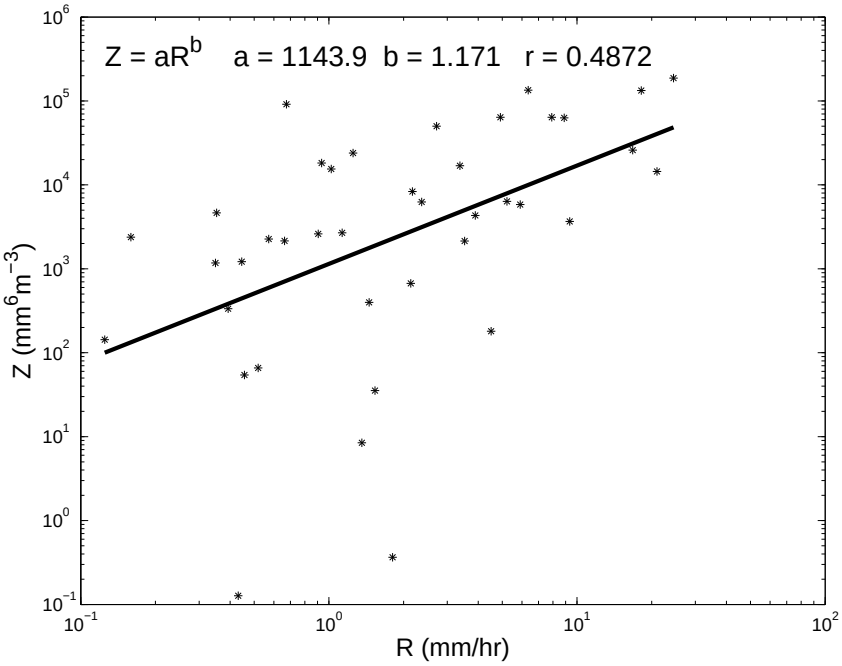

Figure 19: Experimental R-Z relationship developed for KMLB WSR-88D station at the disdrometer location. Data were averaged over one hour periods, and were only included if R was > 0.1 mm/hr.

distribution of points. The 25 km radar method has a RMS_{log} prediction error of 3.09 mm/hr. For the 75 km radar method, the errors are 4.79 mm/hr for the RMS, and 3.84 mm/hr for the RMS_{log}.

4.5 Lightning only method

The second R estimation method evaluated is a direct relationship between R and a parameter of lightning, the lightning only method. This lightning parameter is selected by strongest r, so F for CG lightning on the 25 km domain is plotted against R, and the best fit curve is used for rain estimation. This relationship has already been presented in Table 6, and both the plot and relationship are presented in Fig. 20.

For this method, the RMS prediction error is 5.43 mm/hr, a smaller error than

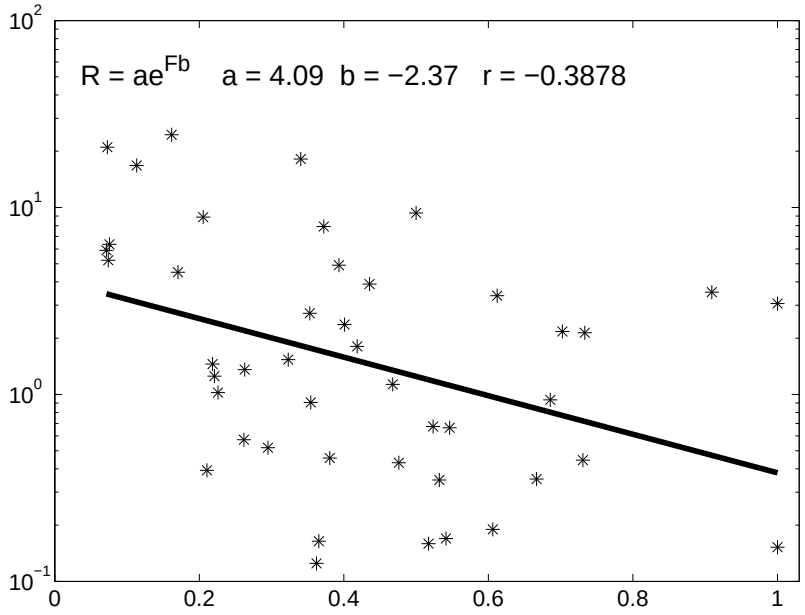

Figure 20: Plot of R and F for CG lightning on the 25 km domain, with best fit exponential relationship. This was the strongest correlation involving R

was found for the radar only method, shown in Fig. 19. The RMS_{log} error, however, is 3.45 mm/hr for the lightning only method, larger than the error for the radar only method.

4.6 Lightning DSD method

The third rain estimation method is to estimate Λ from one lightning parameter, N_0 from a different lightning parameter, and substitute these into Eqs. (5) and (2) to estimate R. From Table 6, Λ is best estimated by $n_{s,a}$ for IC lightning on the 75 km domain, while N_0 is best estimated by $n_{s,a}$ for NBE lightning on the 200 km domain. However, due to differences in the number of data points between these different values of D, both lightning parameters used to estimate DSD parameters must be calculated on the same D. The best estimation parameter, that with the largest r, for N_0 on the 75 km domain will be used, which is $n_{s,a}$ for CG lightning.

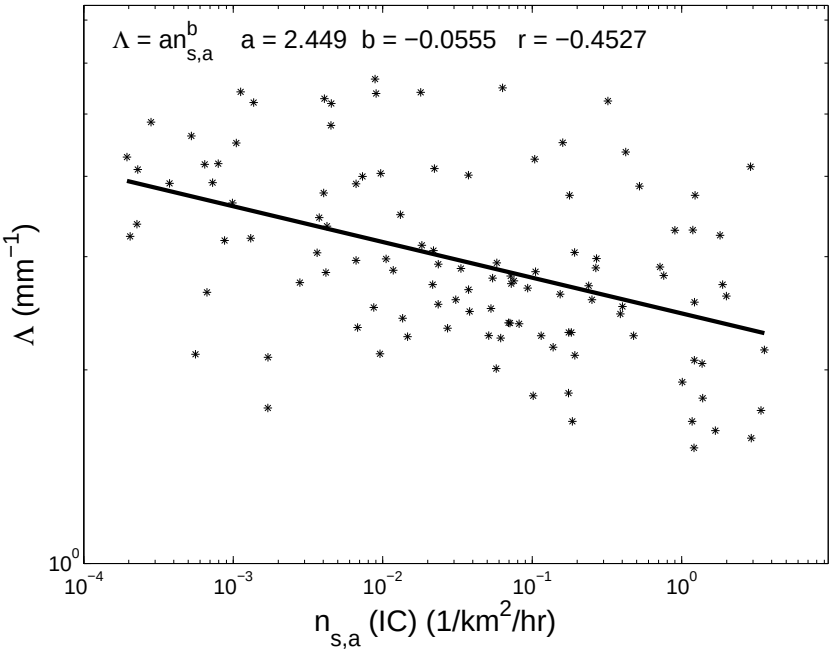

Figure 21: Plot of Λ and IC $n_{s,a}$ on the 75 km domain, the strongest correlation involving Λ. Best fit power law relationship is shown by the solid line.

The two relationships used to estimate DSD parameters are shown in Figs. 21 and 22. Because the relationship used to estimate N_0 is not as well fit as the relationship used to estimate Λ, the majority of the inaccuracies in the lightning DSD method will come from N_0.

Estimates of R are computed with the relationships in Figs. 21 and 22, and compared to actual R. Fig. 23 shows the comparison of the lightning estimated R, and the actual values obtained from the disdrometer data. The RMS error calculated for this method is 5.32 mm/hr. The RMS_{log} error calculated for this method is 6.07 mm/hr. These errors are both much larger than for the 75 km radar method, indicating that the DSD lightning method does not provide an increase in accuracy over radar.

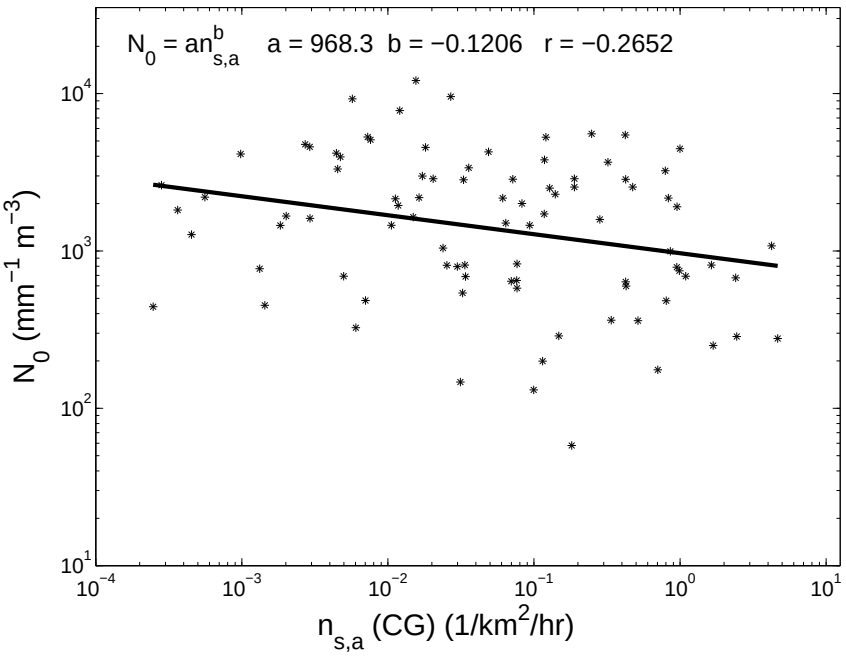

Figure 22: Plot of N_0 and CG $n_{s,a}$ on the 75 km domain, the strongest correlation involving N_0 on the 75 km domain. Best fit power law relationship is shown by the solid line.

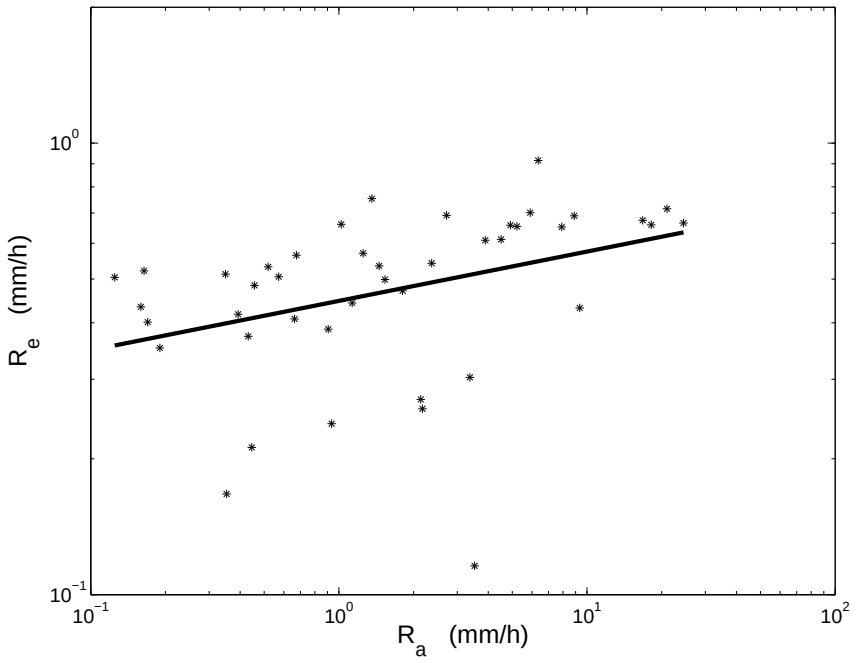

Figure 23: Evaluation of the lightning DSD method. This plot indicates a large amount of scatter about the line of best fit, in comparison to other R estimation methods.

4.7 Radar/lightning method

The final method of rain estimation uses both radar and lightning. It adds lightning data to the current method of estimating R from Z. A multiple regression is performed with R related to both Z and the best lightning estimator of R: F for CG lightning on the 25 km domain. A power law fit is found between R and the first parameter, (Z). Then the second parameter, (F) is fit to the residuals by the use of a linear fit. A linear fit is used for F because some of the residuals are negative, so a exponential fit, as was used previously between R and F is not possible. When combined, the two best fit curves form one equation with four coefficients found by least squares curve fitting:

$$R = aZ^b + cF + d \tag{23}$$

where a, b, c, and d are found by least squares curve fitting, and give a=0.190, b=-1.07, c=-10.86 and d=6.36. Plugging Z and F back into Eq. (23) with these constant values gives estimated values of R from this method. These are compared to the actual values of R in Fig. 24.

The RMS error for the radar/lightning method is 5.06 mm/hr, and the log RMS error is 3.37 mm/hr. When compared to the radar only method, this method exhibits a decline in RMS, but an increase in RMS_{log}.

4.8 Comparison of estimation methods

Tables 7 and 8 summarize the four rain estimation methods evaluated in this work. Because of differences in number of data points, methods should only be compared to those computed for the same D, which are separated in Table 7 for $D = 25$ km, and Table 8 for $D = 75$ km. The radar/lightning method was expected to perform best, because it combines the information in the radar only and lightning only

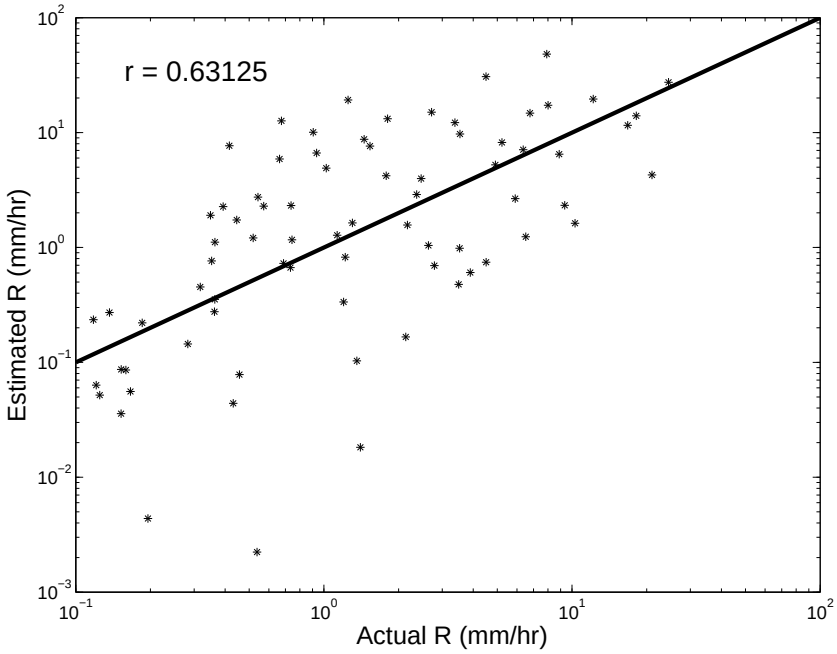

Figure 24: Statistical method of estimating R using a multiple regression with predictors Z and F for CG lightning on the 25 km domain.

Table 7: Summary of the errors produced by the three rain estimation methods studied for $D = 25$ km. For these three methods the mean R was 3.97 mm/hr.

Method	Estimator(s)	RMS error (mm/hr)	RMS_{log} error (mm/hr)
Radar Only (25 km)	Z	5.57	3.09
Lightning Only	F (CG, 25 km)	5.43	3.45
Radar/Lightning	Z & F (CG, 25 km)	5.06	3.37

Table 8: Summary of the errors produced by the two rain estimation methods studied for $D = 75$ km. For these two methods the mean R was 3.12 mm/hr.

Method	Estimator(s)	RMS error (mm/hr)	RMS_{log} error (mm/hr)
Radar Only (75 km)	Z	4.79	3.84
Lightning DSD	$n_{s,a}$ (IC, 75 km) & $n_{s,a}$ (CG,75 km)	5.32	6.07

methods. This result is confirmed by the lower RMS for the radar/lightning method than either radar only or lightning only method. The lightning DSD method produces both a larger RMS and RMS_{log} than the radar only method, meaning it is likely unsuitable for R estimation.

5 DISCUSSION

5.1 Relative strength of lightning and rain parameters

The first objective of this study is to evaluate the relative strength of correlations between rain/lightning parameter pairs. The strongest of these correlations will lead to the best estimation of R, as well as further our understanding of thunderstorm processes. Comparison of these pairs also includes finding the D and lightning type that optimized the correlation.

Many relationships between R and lightning parameters were significant, but the strength of these correlations was less than that for relationships including Λ. The strongest correlation between R and a lightning parameter was between R and F for CG lightning on the 25 km domain, with r = -0.3878. Only CG lightning on the 25 and 50 km domains produced significant correlations between R and F, and r for the relationship on the 50 km domain was much lower than for the 25 km domain. This was a rare result compared to the general trends of correlations in this study. Relationships between a lightning pair were almost always stronger on the 75 or 100 km domain than on the 25 or 50 km domain. Only three cases exhibited a decrease in r with D increasing from 25 km. In addition to the relationship between R and F, the relationship between Λ and F (for CG lightning), and the relationship between N_0 and n_s also exhibited this behavior. Physically, this indicates that the rain parameter is related only to the lightning that is occurring in very close proximity. If r decreases from the 25 to the 50 km domain, then the lightning conditions occurring more than 12.5 km from the rain location are not indicative of the rain being produced. For the majority of rain/lightning parameter pairs, r increased with D to a maximum. This could be due to the lower number of points

for the smaller values of D causing lower r. Physically, this behavior indicates that the lightning activity caused by specific conditions extend 50 km or more from the location of those conditions, but they are not uniform over that area, and the random variations in lightning activity that may exist at the rain location will produce errors is considered. Better results will be obtained if the lightning activity over a large area are averaged.

The implication of this temporal behavior is most significant for the method of using lightning in synergy with radar for rain estimation. To implement this method, which will be discussed later in this section, the value of the lightning parameter would need to be calculated at each location of radar measurement. If a large area is used to calculate the lightning parameter, then its value will change less from point to point than if a smaller area is used. If a large area is used then the resulting R map will be smoothed more, displaying fewer of the temporal variations in R. For this reason, a parameter calculated for a small D, such as 25 km or smaller, may be preferable for use with radar.

The strongest correlations between R and q existed for the largest D of 200 km and for CG lightning, giving $r = 0.3459$. While q for lightning in a close vicinity is poorly correlated to rain, q for lightning across an entire storm cell or system is better related to rain, indicating that temporal variations in lightning may exist, but they have little bearing on the rain at the point of variation. This example is an extreme of the behavior described above, were random variations in lightning activity cause inaccuracies if they are considered, but by averaging lightning over a larger area, a better relationship is found. Because the maximum r was found for the largest D examined, it is possible that the ideal D will be even larger than 200 km. Likewise, it is possible that, for relationships found to be most strongly correlated on the 25 km domain, that the ideal D is actually smaller than 25 km,

although more data would be required to test this. Most relationships displayed an ideal D which was not the largest or smallest examined.

The r for the relationship between R and n_s peaked on the 75 km domain, and was strongest for IC lightning. This relationship had an $r = 0.2939$, and was nearly as strong for total lightning, as it was for IC lightning. Ambiguity exists as to which lightning parameter is best suited to predict R. Although the strongest correlation was between R and F for CG lightning on the 25 km domain with r = -0.3878, on other domains r was much lower or insignificant, suggesting that perhaps this relationship is not completely representative of the true phenomena. The parameters n_s and $n_{s,a}$ produced many significant correlations with R, but had values of r that were lower than others in this study. Also, these parameters only show a slight peak in r at $D = 75$ km, and little difference between lightning type, meaning it is difficult to recommend using a specific D or lightning type, or that these results are more reliable than previous studies which counted lightning regardless of type or location.

Relationships between Λ and lightning parameters were much stronger than those between R and lightning parameters. In general, less scatter was evident in plots including Λ than those including R. Values of r were further from zero, and p-values were smaller. For n_s and $n_{s,a}$, where R produced values of r near 0.3, Λ produced values near -0.45. As with R, the lightning type and D which produced the strongest correlations were the 75 km domain and IC lightning. Relationships between Λ and $n_{s,a}$ were similar to those between Λ and n_s, except that r was slightly stronger for $n_{s,a}$. Relationships between Λ and q performed better than those between R and q, and were best for IC lightning on the 75 km domain.

The most effective parameter for estimating Λ is $n_{s,a}$. For this parameter, a 75 km domain is best, but larger D will work nearly as well because adjusting by radar

information ignores the area of the larger domain which does not contain heavy rain, often treating all domains above a certain size equally. Little difference can be seen between using different lightning types, other than poor performance of NBE lightning on domains smaller than 100 km. The correlation between $n_{s,a}$ for CG lightning and Λ is strongest on the 100 km domain, as opposed to a 75 km domain for IC lightning, meaning CG lightning associated with an area of low Λ likely occurs in a larger surrounding area than IC lightning. These differences are minor, and from a practical standpoint, any lightning type other than NBE can be used, preferably with D between 75 and 125 km.

The DSD parameter N_0 exhibited less scatter in plots than R, but more than Λ . With n_s and $n_{s,a}$, N_0 was best correlated either for small (25 km) D, or large (200 km) D. Correlations on the 10 km domain were ignored due to very few data points. On domains of $D = 100$ km or smaller, N_0 was best correlated with CG lightning n_s, meaning that areas of specific N_0 and CG n_s values are matched on a small area. On domains larger than $D = 100$ km, NBE lightning n_s was most correlated with N_0, so the value of N_0 is related to NBE lightning that occurs over a much larger area than other lightning types. The strongest of these correlations had an r weaker than -0.4, so N_0 is not correlated to n_s or $n_{s,a}$ as well as Λ is correlated to these parameters.

Lightning produces much better estimates of Λ than N_0, so a method which estimates Λ from lightning, and N_0 from some other measurement, such as radar, is likely to perform better than if both are estimated from lightning. If N_0 is to be estimated from lightning, NBE lightning $n_{s,a}$ for a large D (200 km) is the best parameter, although future work should be done on the relationship between n_s and N_0 for a very small D (10 km). This would, however, require a much larger data set, perhaps containing one year or more of storm data.

5.2 Performance of lightning types

It was hypothesized in Section I that rain may be well related to lightning of one type, but not to other lightning types. In general, when one lightning type performed well, others did also, so the hypothesis was disproved. This was especially true for n_s and $n_{s,a}$, which performed only slightly better for IC lightning than total or CG lightning. The main difference between lightning types was not the strength of correlations, but the value of D that produced the best correlations. In the relationship between N_0 and n_s or $n_{s,a}$, it was shown that CG lightning performed best for $D = 100$ km or smaller, and NBE lightning performed best for $D > 100$ km, though the strength of these relationships was similar. This shows that the value N_0, or the intercept of the DSD, is related to the formation of CG lightning on a very local level, while it is related to the formation of NBE lightning on a more regional level. These differences are still much smaller than the differences between different rain/lightning parameter pairs.

In this research, specific interest is given to NBE lightning because of its ease of detection from space. If NBE lightning is strongly correlated to rain, then it would ease the use of satellite based systems for rain estimation. However, few relationships based on NBE lightning were significant, and even fewer were stronger than for other lightning types. This was especially true for direct relationships between R and lightning parameters, where NBE lightning failed to produce any significant correlations. The most promising result for NBE lightning was that $n_{s,a}$ based on this type was much more strongly correlated to N_0 than $n_{s,a}$ for other lightning types. The best estimator of N_0 overall was $n_{s,a}$ for NBE lightning on the 200 km domain. With Λ on the 200 km domain, $n_{s,a}$ for NBE lightning was also fairly well correlated, although less strongly than for other lightning types. NBE lightning would be best used with a large D (200 km) to estimate DSD parameters,

specifically N_0. Although space-based detection of NBE lightning is efficient, using only NBE lightning for rain estimation will likely result in poor performance compared to land based methods with other lightning types.

5.3 Adjusted lightning density

Adjusting lightning density improved many correlations, but only by small margins. This margin increased with D. Often correlations on $D = 50$ km or smaller domains became less significant with $n_{s,a}$ than with n_s, but as D increases, improvements in r with adjustment become larger. However, none of these improvements were enough to draw different conclusions about the best parameters, lightning type, or D to use. Although $n_{s,a}$ is recommended for estimation of Λ and N_0, n_s performs better than other parameters, and should be used even if adjustment by radar is not possible. The conclusion that Λ is best suited for estimation from lightning is valid whether lightning density is adjusted or not.

It was expected that when a storm was covering part of the domain, adjustment would improve the correlation by considering only the area where rain was falling, but leave the same areas when a storm covered the entire domain. It was found, however, that some correlations on domains 50 km and smaller became weaker after adjustment than before, and this effect was amplified as D decreased. A possible explanation is that the area of lightning activity does not directly correspond to the area of radar reflectivity. Lightning activity may be leading, trailing, or otherwise offset from radar reflectivity. Some research has found that the core of lightning activity does not correspond to the core of precipitation[2, 14], although other research has found that the cores do correspond[11, 27]. We interpret our data as supporting a lack of superposition of the core of lightning activity and the core of precipitation.

5.4 Comparison of R estimation methods

Comparison of the four methods of estimation of R is somewhat difficult because of the use of different D, which leads to different numbers of data points, and the two measures of estimation accuracy, RMS and RMS_{log}. This section will attempt to clarify the relative performance of the different methods.

The first observation is that the lightning DSD method is a poor estimator of R. This is seen clearly in Fig. 23, where the trend of the estimated data has a very small slope, causing overestimation at low values of R (0.1 mm/hr), and underestimation at high values of R (10 mm/hr). The RMS error of this method is comparable to that of other methods, because the main component of the RMS error in most situations studied here is the overestimation at a few high R points, which does not occur for the DSD method. The RMS_{log}, however, is much higher for this method than any other, showing the poor quality of this trend.

From the results presented here it can not be recommended that the lightning DSD method be used for rain estimation. The correlation results for the DSD parameters may be very useful for the understanding of thunderstorm physics, and possibly lead to advancements in R estimation. The method examined in this work does not perform as well as either the radar only method, or the lightning only method.

The lightning only method performed much better than the lightning DSD method. The lightning DSD method performed worse than the radar only method for the same D, while the lightning only method performed better than the radar only method. The lightning only method also performed much better when comparing the RMS_{log} of the two, which was nearly half for the lightning only method compared to the DSD lightning method.

The lightning only method and the radar only method result in similar

accuracy. The direct lightning method has a slightly lower RMS error, but a slightly higher RMS_{log}, though the differences were small ($< 10\%$), so these methods result in comparable accuracy. A lightning only method is not advisable as a complete replacement for radar, because radar will have resolution for stratiform rain, or other periods without lightning. Even during thunderstorm conditions, the use of lightning instead of radar will not lead to large improvements in accuracy, so the conversion from a radar method to a lightning method may not be worthwhile. Lightning will be more useful for new rain estimation capability where none exists, or especially where ground radar or lightning detection networks are not possible, and satellite detection must be used. In these cases, the methods can be evaluated on cost or other factors, because they are comparable in accuracy. With current radar networks, lightning may be used as a proxy when radar information is not available, such as in areas where buildings or terrain obstruct radar signals, or when stations are inoperable due to repairs. Further studies should be performed to evaluate the long-term accuracy of a lightning only method, in comparison with radar.

5.5 Rain estimation using a combined radar/lightning model

The final rain estimation method uses a combination of radar and lightning, and R is computed by statistical best fit curves to these parameters. This method does improve on the radar method in terms of RMS error, but the radar only method is better in terms of RMS_{log}. This may be due to the addition of the lightning, which was done in the linear space, causing the relationship to be optimized for the linear RMS but not the log-space RMS_{log}. The differences in either RMS between this radar/lightning method and the radar method are small, so lightning, used in this way, will not be likely to lead to large improvements in R estimation accuracy.

Which method is preferable, however, may hinge on the opinion of which error method, the RMS or the RMS_{log} is more appropriate for the situation. For example, in flood warning, large percentage errors may be allowable at low R, but not at high R. For example, a difference between 1 and 2 mm/hr will not cause a difference in flood warnings, but a difference between 10 and 20 mm/hr will cause large difference. In this case, the RMS would be the advisable parameter to follow.

The radar/lightning method should be further studied because of the promise of results shown here, and its ease of application, should a situation be found where it will provide improved accuracy. NLDN currently provides lightning data for the continental United States with real-time access. To implement a radar/lightning method for estimation of R, first a relation must be found between R and Z and a parameter of lightning. Then at the location of radar-data processing, NLDN data, or data from another lightning detection network must be implemented. At each location of Z measurement, NLDN data must be used to find lightning that occurred in the specific domain around the Z location. This is used to calculate the lightning parameter which is used in addition to Z to estimate R. This process should be possible with minimal changes to hardware facilities, and the additional processing power required for these calculations would likely be negligible compared to current processing of radar data.

It may be found that this method is particularly useful in areas where portions of the signal are blocked by terrain, or where radar measurements are known to be inaccurate. These situations should be studied individually for improvements by using lightning information in addition to radar, with a data set comprising a long period of time, up to one year or more. This work suggests that F for CG lightning is the best parameter to calculate from lightning, but this could be site specific, and multiple parameters and values of D should be examined for each case.

6 CONCLUSION

This study included two primary objectives. For the first, which was to determine the strength of correlation between several lightning and rain parameters, parameters of lightning were related to parameters of rain, and evaluated on the strength of correlation. For the second objective, which was to determine which rain estimation method is most accurate, four methods of estimating R by either radar, lightning, or a combination of the two, were evaluated by the RMS error. Results of this study further the understanding of the physical processes which create lightning and rain within convective activity, and lead future research and applications for estimation of R.

To achieve the first objective, four parameters of lightning, n_s, $n_{s,a}$, q, and F, were each examined for correlations with R and the two parameters of the exponential DSD, Λ, and N_0. These analyses were performed for each of three lightning types, IC, CG, and NBE, and for lightning observed in several D surrounding the rain measurement location. Relationships analyzed in this study ranged from no correlation to near r=0.5 in strength. The strongest relationship occurred between Λ and $n_{s,a}$, specifically for IC lightning observed on a 75 km domain. Correlations between lightning parameters and R were found, though these were not as strong as those with Λ . They do, however, permit a direct method of estimating R from lightning. The lightning parameter most strongly correlated to R was F for CG lightning on the 25 km domain. Significant correlations were also observed between lightning parameters and N_0, although they were generally less significant than those with either R or Λ. NBE lightning was given special consideration for its efficiency in detection from space, but was found to be poorly

correlated to most rain parameters, compared to other lightning types.

To achieve the second objective, four methods of estimating R were examined: radar only, lightning only, lightning DSD, and a combined radar/lightning method. The radar only method, is analogous to the currently used method of real-time remote sensing of R, and gives a baseline for performance of the other methods. The lightning only method was found to have comparable accuracy to the radar only method, providing a suitable alternative to radar in certain situations, such as locations without radar coverage, or when existing radar is inoperable. The lightning DSD method, was found to be inaccurate, with estimated values of R all near a general mean, regardless of actual R. The final method, the radar/lightning method, performed similarly to the radar only method, with little apparent increase in accuracy. This final method should be further studied, because, although it showed little improvement in accuracy here, it may have a greater effect in locations where radar is more commonly obstructed or known to have inaccuracies.

APPENDIX: DETAILED CORRELATION RESULTS

Table A-1: Relationships between R and n_s.

D	Total Lightning	CG Lightning	IC Lightning	NBE Lightning
25	0.1249 (0.2924) $R = 1.9209n_s^{0.0772}$	0.0260 (0.8653) $R = 1.5857n_s^{0.0225}$	0.1671 (0.1637) $R = 2.1961n_s^{0.1085}$	0.1683 (0.3195) $R = 4.4327n_s^{0.2016}$
50	0.2663 (0.0071) $R = 1.9425n_s^{0.1408}$	0.0630 (0.5936) $R = 1.6159n_s^{0.0416}$	0.2925 (0.0030) $R = 2.2162n_s^{0.1613}$	0.0461 (0.7357) $R = 2.1282n_s^{0.0406}$
75	0.2745 (0.0031) $R = 1.7896n_s^{0.1371}$	0.1841 (0.0842) $R = 1.7959n_s^{0.1061}$	0.2939 (0.0015) $R = 2.0316n_s^{0.1558}$	0.0322 (0.7896) $R = 1.8281n_s^{0.0253}$
100	0.2395 (0.0096) $R = 1.6472n_s^{0.1190}$	0.1987 (0.0464) $R = 1.6962n_s^{0.1026}$	0.2550 (0.0057) $R = 1.8393n_s^{0.1341}$	0.0694 (0.5410) $R = 1.9404n_s^{0.0495}$
125	0.2284 (0.0121) $R = 1.5672n_s^{0.1106}$	0.1375 (0.1619) $R = 1.5212n_s^{0.0705}$	0.2305 (0.0117) $R = 1.7148n_s^{0.1210}$	-0.0094 (0.9321) $R = 1.3989n_s^{-0.0064}$
150	0.2328 (0.0090) $R = 1.5397n_s^{0.1084}$	0.1564 (0.1045) $R = 1.5241n_s^{0.0801}$	0.2459 (0.0057) $R = 1.7074n_s^{0.1220}$	0.0549 (0.6053) $R = 1.6792n_s^{0.0365}$
175	0.2227 (0.0125) $R = 1.5294n_s^{0.1062}$	0.1596 (0.0959) $R = 1.5293n_s^{0.0827}$	0.2344 (0.0085) $R = 1.6945n_s^{0.1191}$	0.0721 (0.4944) $R = 1.7752n_s^{0.0477}$
200	0.2208 (0.0133) $R = 1.5351n_s^{0.1083}$	0.1973 (0.0354) $R = 1.5874n_s^{0.0993}$	0.2397 (0.0071) $R = 1.7277n_s^{0.1247}$	0.0829 (0.4247) $R = 1.8336n_s^{0.0539}$

Table A-2: Relationships between R and $n_{s,a}$.

D	Total Lightning	CG Lightning	IC Lightning	NBE Lightning
25	0.0861 (0.4691) $R = 1.8094n_{s,a}^{0.0542}$	-0.0292 (0.8489) $R = 1.4293n_{s,a}^{-0.0259}$	0.1225 (0.3088) $R = 2.0228n_{s,a}^{0.0804}$	0.0802 (0.6368) $R = 2.6551n_{s,a}^{0.0957}$
50	0.2625 (0.0080) $R = 1.8725n_{s,a}^{0.1416}$	0.0579 (0.6244) $R = 1.5863n_{s,a}^{0.0390}$	0.2894 (0.0033) $R = 2.1327n_{s,a}^{0.1633}$	0.0251 (0.8543) $R = 1.9207n_{s,a}^{0.0225}$
75	0.2806 (0.0025) $R = 1.7213n_{s,a}^{0.1447}$	0.1905 (0.0737) $R = 1.7566n_{s,a}^{0.1131}$	0.3013 (0.0011) $R = 1.9562n_{s,a}^{0.1654}$	0.0359 (0.7661) $R = 1.8491n_{s,a}^{0.0293}$
100	0.2593 (0.0049) $R = 1.6035n_{s,a}^{0.1344}$	0.2041 (0.0406) $R = 1.6384n_{s,a}^{0.1091}$	0.2771 (0.0026) $R = 1.8058n_{s,a}^{0.1528}$	0.0960 (0.3972) $R = 2.1285n_{s,a}^{0.0716}$
125	0.2597 (0.0042) $R = 1.5302n_{s,a}^{0.1282}$	0.1632 (0.0962) $R = 1.5282n_{s,a}^{0.0864}$	0.2646 (0.0036) $R = 1.6910n_{s,a}^{0.1418}$	0.0199 (0.8565) $R = 1.5619n_{s,a}^{0.0141}$
150	0.2693 (0.0024) $R = 1.4957n_{s,a}^{0.1263}$	0.1919 (0.0456) $R = 1.5340n_{s,a}^{0.1008}$	0.2843 (0.0013) $R = 1.6666n_{s,a}^{0.1420}$	0.0892 (0.4003) $R = 1.8647n_{s,a}^{0.0605}$
175	0.2650 (0.0028) $R = 1.4835n_{s,a}^{0.1264}$	0.2010 (0.0353) $R = 1.5389n_{s,a}^{0.1068}$	0.2790 (0.0016) $R = 1.6542n_{s,a}^{0.1416}$	0.1079 (0.3061) $R = 1.9576n_{s,a}^{0.0723}$
200	0.2651 (0.0028) $R = 1.4751n_{s,a}^{0.1289}$	0.2459 (0.0084) $R = 1.5760n_{s,a}^{0.1242}$	0.2855 (0.0012) $R = 1.6600n_{s,a}^{0.1466}$	0.1170 (0.2587) $R = 1.9899n_{s,a}^{0.0772}$

Table A-3: Relationships between R and q.

D	Total Lightning	CG Lightning	IC Lightning	NBE Lightning
25	0.0980 (0.4093) $R = 1.137exp^{0.4742q}$	0.3022 (0.0436) $R = 0.716exp^{1.421q}$	-0.0174 (0.8856) $R = 1.766exp^{-0.0970q}$	-0.0695 (0.6827) $R = 2.235exp^{-0.3561q}$
50	-0.0124 (0.9018) $R = 1.308exp^{-0.0688q}$	0.1318 (0.2631) $R = 0.997exp^{0.6125q}$	-0.0690 (0.4928) $R = 1.700exp^{-0.3926q}$	-0.1449 (0.2867) $R = 3.082exp^{-0.7541q}$
75	0.2042 (0.0294) $R = 0.496exp^{1.212q}$	0.1360 (0.2038) $R = 0.851exp^{0.6827q}$	0.2038 (0.0296) $R = 0.447exp^{1.216q}$	-0.0548 (0.6500) $R = 1.922exp^{-0.2616q}$
100	0.2639 (0.0042) $R = 0.287exp^{1.936q}$	0.1858 (0.0629) $R = 0.659exp^{0.9575q}$	0.2776 (0.0026) $R = 0.238exp^{2.001q}$	-0.0246 (0.8283) $R = 1.643exp^{-0.1488q}$
125	0.2156 (0.0181) $R = 0.318exp^{1.728q}$	0.1386 (0.1584) $R = 0.716exp^{0.8143q}$	0.2480 (0.0065) $R = 0.233exp^{1.971q}$	0.1112 (0.3108) $R = 0.856exp^{0.6725q}$
150	0.1767 (0.0486) $R = 0.364exp^{1.473q}$	0.2772 (0.0035) $R = 0.469exp^{1.583q}$	0.1626 (0.0701) $R = 0.302exp^{1.538q}$	-0.0176 (0.8681) $R = 1.499exp^{-0.1364q}$
175	0.1828 (0.0413) $R = 0.345exp^{1.554q}$	0.3075 (0.0011) $R = 0.396exp^{1.896q}$	0.1448 (0.1071) $R = 0.346exp^{1.369q}$	-0.0528 (0.6175) $R = 1.848exp^{-0.4194q}$
200	0.2286 (0.0103) $R = 0.299exp^{1.813q}$	0.3459 (0.0002) $R = 0.370exp^{2.080q}$	0.1641 (0.0675) $R = 0.323exp^{1.472q}$	-0.0277 (0.7900) $R = 1.535exp^{-0.2079q}$

Table A-4: Relationships between R and F.

D	CG Lightning	IC Lightning	NBE Lightning
25	-0.3878 (0.0085) $R = 4.090exp^{-2.3734F}$	0.2237 (0.0608) $R = 0.653exp^{1.2202F}$	0.0283 (0.8678) $R = 1.6014exp^{2.0559F}$
50	-0.2777 (0.0166) $R = 3.0429exp^{-2.0286F}$	0.0494 (0.6235) $R = 1.0108exp^{0.2920F}$	-0.0419 (0.7590) $R = 1.8194exp^{-2.5638F}$
75	-0.1829 (0.0862) $R = 2.2929exp^{-1.6405F}$	-0.0016 (0.9864) $R = 1.1408exp^{-0.0112F}$	-0.0789 (0.5130) $R = 1.7359exp^{-3.5037F}$
100	-0.0823 (0.4131) $R = 1.5182exp^{-0.7082F}$	-0.0066 (0.9437) $R = 1.1639exp^{-0.0479F}$	0.1144 (0.3123) $R = 1.2184exp^{7.4382F}$
125	-0.0758 (0.4422) $R = 1.4999exp^{-0.6793F}$	-0.0786 (0.3956) $R = 1.6542exp^{-0.6136F}$	0.1123 (0.3061) $R = 1.2020exp^{7.6425F}$
150	-0.0615 (0.5254) $R = 1.4013exp^{-0.6062F}$	-0.0576 (0.5232) $R = 1.4140exp^{-0.4467F}$	0.1337 (0.2063) $R = 1.0610exp^{10.7765F}$
175	-0.0503 (0.6019) $R = 1.3327exp^{-0.4789F}$	-0.0540 (0.5494) $R = 1.3741exp^{-0.4118F}$	0.1549 (0.1405) $R = 1.0179exp^{12.5527F}$
200	-0.1002 (0.2887) $R = 1.5403exp^{-0.9766F}$	0.0395 (0.6621) $R = 0.8586exp^{0.3192F}$	0.1583 (0.1256) $R = 0.9860exp^{13.8514F}$

Table A-5: Relationships between Λ and n_s.

D	Total Lightning	CG Lightning	IC Lightning	NBE Lightning
25	-0.3254 (0.0050) $\Lambda = 2.4449 n_s^{-0.0451}$	-0.2897 (0.0535) $\Lambda = 2.3549 n_s^{-0.0596}$	-0.3670 (0.0016) $\Lambda = 2.3364 n_s^{-0.0524}$	-0.2983 (0.0729) $\Lambda = 1.6938 n_s^{-0.0795}$
50	-0.3708 (0.0001) $\Lambda = 2.4893 n_s^{-0.0443}$	-0.2787 (0.0162) $\Lambda = 2.4244 n_s^{-0.0413}$	-0.3965 (0.0000) $\Lambda = 2.3996 n_s^{-0.0494}$	-0.2009 (0.1376) $\Lambda = 2.1132 n_s^{-0.0359}$
75	-0.4149 (0.0000) $\Lambda = 2.5206 n_s^{-0.0463}$	-0.3586 (0.0006) $\Lambda = 2.4325 n_s^{-0.0459}$	-0.4269 (0.0000) $\Lambda = 2.4337 n_s^{-0.0506}$	-0.1611 (0.1796) $\Lambda = 2.2769 n_s^{-0.0266}$
100	-0.3820 (0.0000) $\Lambda = 2.5700 n_s^{-0.0422}$	-0.3766 (0.0001) $\Lambda = 2.4799 n_s^{-0.0438}$	-0.3910 (0.0000) $\Lambda = 2.4881 n_s^{-0.0457}$	-0.2102 (0.0613) $\Lambda = 2.2612 n_s^{-0.0308}$
125	-0.3666 (0.0000) $\Lambda = 2.6073 n_s^{-0.0390}$	-0.3296 (0.0006) $\Lambda = 2.5409 n_s^{-0.0373}$	-0.3739 (0.0000) $\Lambda = 2.5244 n_s^{-0.0431}$	-0.2112 (0.0524) $\Lambda = 2.3020 n_s^{-0.0294}$
150	-0.3619 (0.0000) $\Lambda = 2.6261 n_s^{-0.0374}$	-0.2969 (0.0017) $\Lambda = 2.5782 n_s^{-0.0333}$	-0.3740 (0.0000) $\Lambda = 2.5429 n_s^{-0.0412}$	-0.2996 (0.0039) $\Lambda = 2.1637 n_s^{-0.0433}$
175	-0.3487 (0.0001) $\Lambda = 2.6298 n_s^{-0.0369}$	-0.3046 (0.0012) $\Lambda = 2.5710 n_s^{-0.0349}$	-0.3602 (0.0000) $\Lambda = 2.5454 n_s^{-0.0407}$	-0.3145 (0.0023) $\Lambda = 2.1293 n_s^{-0.0457}$
200	-0.3453 (0.0001) $\Lambda = 2.6266 n_s^{-0.0376}$	-0.3041 (0.0010) $\Lambda = 2.5787 n_s^{-0.0344}$	-0.3655 (0.0000) $\Lambda = 2.5320 n_s^{-0.0422}$	-0.3219 (0.0015) $\Lambda = 2.1128 n_s^{-0.0469}$

Table A-6: Relationships between Λ and $n_{s,a}$.

D	Total Lightning	CG Lightning	IC Lightning	NBE Lightning
25	-0.3070 (0.0083) $\Lambda = 2.4633 n_{s,a}^{-0.0433}$	-0.2487 (0.0995) $\Lambda = 2.3967 n_{s,a}^{-0.0524}$	-0.3450 (0.0032) $\Lambda = 2.3610 n_{s,a}^{-0.0498}$	-0.2715 (0.1041) $\Lambda = 1.7603 n_{s,a}^{-0.0720}$
50	-0.3887 (0.0001) $\Lambda = 2.4975 n_{s,a}^{-0.0474}$	-0.2773 (0.0168) $\Lambda = 2.4459 n_{s,a}^{-0.0419}$	-0.4163 (0.0000) $\Lambda = 2.4037 n_{s,a}^{-0.0531}$	-0.2271 (0.0923) $\Lambda = 2.0709 n_{s,a}^{-0.0414}$
75	-0.4385 (0.0000) $\Lambda = 2.5416 n_{s,a}^{-0.0506}$	-0.3894 (0.0002) $\Lambda = 2.4383 n_{s,a}^{-0.0513}$	-0.4527 (0.0000) $\Lambda = 2.4486 n_{s,a}^{-0.0555}$	-0.2301 (0.0536) $\Lambda = 2.1503 n_{s,a}^{-0.0395}$
100	-0.4194 (0.0000) $\Lambda = 2.5901 n_{s,a}^{-0.0483}$	-0.4084 (0.0000) $\Lambda = 2.4968 n_{s,a}^{-0.0492}$	-0.4318 (0.0000) $\Lambda = 2.4973 n_{s,a}^{-0.0529}$	-0.2938 (0.0082) $\Lambda = 2.1295 n_{s,a}^{-0.0450}$
125	-0.4108 (0.0000) $\Lambda = 2.6337 n_{s,a}^{-0.0445}$	-0.3754 (0.0001) $\Lambda = 2.5493 n_{s,a}^{-0.0439}$	-0.4220 (0.0000) $\Lambda = 2.5434 n_{s,a}^{-0.0497}$	-0.2853 (0.0081) $\Lambda = 2.2027 n_{s,a}^{-0.0414}$
150	-0.4100 (0.0000) $\Lambda = 2.6591 n_{s,a}^{-0.0427}$	-0.3511 (0.0002) $\Lambda = 2.5834 n_{s,a}^{-0.0404}$	-0.4246 (0.0000) $\Lambda = 2.5710 n_{s,a}^{-0.0471}$	-0.3730 (0.0003) $\Lambda = 2.0928 n_{s,a}^{-0.0550}$
175	-0.4024 (0.0000) $\Lambda = 2.6674 n_{s,a}^{-0.0426}$	-0.3630 (0.0001) $\Lambda = 2.5834 n_{s,a}^{-0.0426}$	-0.4166 (0.0000) $\Lambda = 2.5777 n_{s,a}^{-0.0470}$	-0.3875 (0.0001) $\Lambda = 2.0732 n_{s,a}^{-0.0571}$
200	-0.4020 (0.0000) $\Lambda = 2.6730 n_{s,a}^{-0.0434}$	-0.3697 (0.0001) $\Lambda = 2.5940 n_{s,a}^{-0.0420}$	-0.4238 (0.0000) $\Lambda = 2.5769 n_{s,a}^{-0.0483}$	-0.3923 (0.0001) $\Lambda = 2.0705 n_{s,a}^{-0.0581}$

Table A-7: Relationships between Λ and q.

D	Total Lightning	CG Lightning	IC Lightning	NBE Lightning
25	-0.1119 (0.3461) $\Lambda = 2.972exp^{-0.1213q}$	-0.2558 (0.0899) $\Lambda = 3.114exp^{-0.2862q}$	0.0483 (0.6889) $\Lambda = 2.570exp^{0.0594q}$	-0.0642 (0.7057) $\Lambda = 2.632exp^{-0.0732q}$
50	-0.0833 (0.4076) $\Lambda = 3.092exp^{-0.1043q}$	-0.1771 (0.1313) $\Lambda = 3.071exp^{-0.1847q}$	-0.0526 (0.6013) $\Lambda = 3.023exp^{-0.0676q}$	-0.0345 (0.8004) $\Lambda = 2.639exp^{-0.0365q}$
75	-0.2771 (0.0028) $\Lambda = 3.778exp^{-0.3675q}$	-0.1379 (0.1974) $\Lambda = 3.101exp^{-0.1536q}$	-0.3070 (0.0009) $\Lambda = 4.022exp^{-0.4092q}$	0.0043 (0.9715) $\Lambda = 2.633exp^{0.0043q}$
100	-0.3077 (0.0008) $\Lambda = 4.188exp^{-0.5018q}$	-0.1163 (0.2466) $\Lambda = 3.153exp^{-0.1352q}$	-0.3766 (0.0000) $\Lambda = 4.699exp^{-0.6034q}$	-0.0857 (0.4495) $\Lambda = 2.930exp^{-0.1063q}$
125	-0.2249 (0.0135) $\Lambda = 3.929exp^{-0.3958q}$	-0.0186 (0.8503) $\Lambda = 2.963exp^{-0.0242q}$	-0.3090 (0.0006) $\Lambda = 4.517exp^{-0.5391q}$	-0.2384 (0.0280) $\Lambda = 3.445exp^{-0.2957q}$
150	-0.1490 (0.0973) $\Lambda = 3.653exp^{-0.2759q}$	-0.2056 (0.0320) $\Lambda = 3.376exp^{-0.2572q}$	-0.1879 (0.0359) $\Lambda = 4.125exp^{-0.3951q}$	-0.0946 (0.3723) $\Lambda = 3.203exp^{-0.1591q}$
175	-0.2023 (0.0237) $\Lambda = 3.937exp^{-0.3821q}$	-0.2722 (0.0040) $\Lambda = 3.600exp^{-0.3707q}$	-0.1902 (0.0336) $\Lambda = 4.140exp^{-0.3997q}$	-0.0471 (0.6557) $\Lambda = 3.034exp^{-0.0823q}$
200	-0.2559 (0.0040) $\Lambda = 4.095exp^{-0.4511q}$	-0.2937 (0.0015) $\Lambda = 3.625exp^{-0.3968q}$	-0.2170 (0.0151) $\Lambda = 4.235exp^{-0.4328q}$	-0.0928 (0.3711) $\Lambda = 3.239exp^{-0.1563q}$

Table A-8: Relationships between Λ and F.

D	CG Lightning	IC Lightning	NBE Lightning
25	0.4391 (0.0025) $\Lambda = 2.0487exp^{0.6394F}$	-0.1060 (0.3789) $\Lambda = 2.9671exp^{-0.1273F}$	-0.0356 (0.8341) $\Lambda = 2.5163exp^{-0.5750F}$
50	0.2668 (0.0216) $\Lambda = 2.3436exp^{0.4372F}$	-0.0114 (0.9100) $\Lambda = 2.8950exp^{-0.0152F}$	0.0484 (0.7231) $\Lambda = 2.5277exp^{0.6010F}$
75	0.0707 (0.5103) $\Lambda = 2.6996exp^{0.1407F}$	0.1334 (0.1572) $\Lambda = 2.5490exp^{0.2064F}$	-0.0019 (0.9873) $\Lambda = 2.6424exp^{-0.0180F}$
100	-0.0404 (0.6880) $\Lambda = 2.9937exp^{-0.0784F}$	0.1088 (0.2450) $\Lambda = 2.6188exp^{0.1747F}$	-0.0304 (0.7887) $\Lambda = 2.7232exp^{-0.4063F}$
125	-0.0000 (0.9997) $\Lambda = 2.9200exp^{-0.0001F}$	0.1320 (0.1525) $\Lambda = 2.5436exp^{0.2262F}$	-0.0558 (0.6120) $\Lambda = 2.7843exp^{-0.7788F}$
150	-0.0159 (0.8696) $\Lambda = 2.9683exp^{-0.0344F}$	0.1513 (0.0922) $\Lambda = 2.5209exp^{0.2604F}$	-0.1090 (0.3038) $\Lambda = 2.9394exp^{-1.9099F}$
175	-0.0154 (0.8731) $\Lambda = 2.9802exp^{-0.0324F}$	0.1300 (0.1483) $\Lambda = 2.5969exp^{0.2201F}$	-0.1420 (0.1770) $\Lambda = 2.9883exp^{-2.5293F}$
200	0.0751 (0.4271) $\Lambda = 2.7843exp^{0.1645F}$	0.0282 (0.7552) $\Lambda = 2.9000exp^{0.0506F}$	-0.1409 (0.1731) $\Lambda = 3.0159exp^{-2.7671F}$

Table A-9: Relationships between N_0 and n_s.

D	Total Lightning	CG Lightning	IC Lightning	NBE Lightning
25	-0.2434 (0.0380) $N_0 = 1079n_s^{-0.1240}$	-0.3200 (0.0321) $N_0 = 762n_s^{-0.2400}$	-0.2335 (0.0500) $N_0 = 1003n_s^{-0.1260}$	-0.1617 (0.3390) $N_0 = 478n_s^{-0.1550}$
50	-0.1537 (0.1250) $N_0 = 1173n_s^{-0.0610}$	-0.2741 (0.0181) $N_0 = 876n_s^{-0.1420}$	-0.1550 (0.1217) $N_0 = 1131n_s^{-0.0650}$	-0.1655 (0.2230) $N_0 = 626n_s^{-0.1170}$
75	-0.2113 (0.0240) $N_0 = 1139n_s^{-0.0770}$	-0.2329 (0.0281) $N_0 = 979n_s^{-0.1020}$	-0.2020 (0.0312) $N_0 = 1098n_s^{-0.0780}$	-0.1430 (0.2342) $N_0 = 753n_s^{-0.0900}$
100	-0.2076 (0.0254) $N_0 = 1147n_s^{-0.0760}$	-0.2504 (0.0116) $N_0 = 1007n_s^{-0.0980}$	-0.1994 (0.0319) $N_0 = 1102n_s^{-0.0770}$	-0.1664 (0.1403) $N_0 = 758n_s^{-0.0900}$
125	-0.1979 (0.0302) $N_0 = 1164n_s^{-0.0700}$	-0.2576 (0.0080) $N_0 = 1013n_s^{-0.0990}$	-0.2051 (0.0253) $N_0 = 1096n_s^{-0.0790}$	-0.2692 (0.0127) $N_0 = 592n_s^{-0.1400}$
150	-0.1942 (0.0300) $N_0 = 1183n_s^{-0.0660}$	-0.1916 (0.0459) $N_0 = 1082n_s^{-0.0720}$	-0.1939 (0.0303) $N_0 = 1128n_s^{-0.0700}$	-0.3208 (0.0019) $N_0 = 533n_s^{-0.1610}$
175	-0.1893 (0.0344) $N_0 = 1182n_s^{-0.0660}$	-0.2005 (0.0357) $N_0 = 1072n_s^{-0.0770}$	-0.1900 (0.0338) $N_0 = 1124n_s^{-0.0700}$	-0.3248 (0.0016) $N_0 = 522n_s^{-0.1610}$
200	-0.1873 (0.0365) $N_0 = 1180n_s^{-0.0670}$	-0.1576 (0.0940) $N_0 = 1127n_s^{-0.0590}$	-0.1903 (0.0335) $N_0 = 1118n_s^{-0.0720}$	-0.3294 (0.0011) $N_0 = 515n_s^{-0.1630}$

Table A-10: Relationships between N_0 and $n_{s,a}$.

D	Total Lightning	CG Lightning	IC Lightning	NBE Lightning
25	-0.2661 (0.0229) $N_0 = 1053n_{s,a}^{-0.1380}$	-0.3293 (0.0272) $N_0 = 748n_{s,a}^{-0.2530}$	-0.2587 (0.0294) $N_0 = 971n_{s,a}^{-0.1420}$	-0.2339 (0.1635) $N_0 = 346n_{s,a}^{-0.2240}$
50	-0.1830 (0.0670) $N_0 = 1149n_{s,a}^{-0.0750}$	-0.2778 (0.0166) $N_0 = 896n_{s,a}^{-0.1470}$	-0.1859 (0.0627) $N_0 = 1096n_{s,a}^{-0.0790}$	-0.2204 (0.1027) $N_0 = 517n_{s,a}^{-0.1590}$
75	-0.2361 (0.0114) $N_0 = 1139n_{s,a}^{-0.0890}$	-0.2652 (0.0120) $N_0 = 967n_{s,a}^{-0.1200}$	-0.2282 (0.0146) $N_0 = 1088n_{s,a}^{-0.0920}$	-0.2197 (0.0656) $N_0 = 588n_{s,a}^{-0.1440}$
100	-0.2328 (0.0119) $N_0 = 1157n_{s,a}^{-0.0890}$	-0.2865 (0.0037) $N_0 = 1003n_{s,a}^{-0.1160}$	-0.2262 (0.0146) $N_0 = 1101n_{s,a}^{-0.0920}$	-0.2346 (0.0362) $N_0 = 632n_{s,a}^{-0.1330}$
125	-0.2171 (0.0172) $N_0 = 1191n_{s,a}^{-0.0790}$	-0.2857 (0.0031) $N_0 = 1031n_{s,a}^{-0.1130}$	-0.2259 (0.0135) $N_0 = 1118n_{s,a}^{-0.0890}$	-0.3216 (0.0027) $N_0 = 540n_{s,a}^{-0.1740}$
150	-0.2128 (0.0172) $N_0 = 1218n_{s,a}^{-0.0730}$	-0.2181 (0.0227) $N_0 = 1097n_{s,a}^{-0.0850}$	-0.2132 (0.0170) $N_0 = 1159n_{s,a}^{-0.0770}$	-0.3718 (0.0003) $N_0 = 508n_{s,a}^{-0.1910}$
175	-0.2078 (0.0201) $N_0 = 1225n_{s,a}^{-0.0720}$	-0.2252 (0.0180) $N_0 = 1102n_{s,a}^{-0.0890}$	-0.2093 (0.0192) $N_0 = 1164n_{s,a}^{-0.0770}$	-0.3747 (0.0002) $N_0 = 510n_{s,a}^{-0.1890}$
200	-0.2071 (0.0205) $N_0 = 1230n_{s,a}^{-0.0730}$	-0.1844 (0.0495) $N_0 = 1148n_{s,a}^{-0.0690}$	-0.2106 (0.0184) $N_0 = 1166n_{s,a}^{-0.0790}$	-0.3792 (0.0002) $N_0 = 511n_{s,a}^{-0.1900}$

Table A-11: Relationships between N_0 and q.

D	Total Lightning	CG Lightning	IC Lightning	NBE Lightning
25	-0.0151 (0.8993) $N_0 = 1522exp^{-0.060q}$	0.0241 (0.8751) $N_0 = 1218exp^{0.098q}$	0.0479 (0.6916) $N_0 = 1183exp^{0.223q}$	-0.1584 (0.3491) $N_0 = 1702exp^{-0.652q}$
50	-0.1313 (0.1906) $N_0 = 2143exp^{-0.554q}$	-0.0735 (0.5337) $N_0 = 1608exp^{-0.269q}$	-0.1608 (0.1083) $N_0 = 2487.exp^{-0.696q}$	-0.2171 (0.1080) $N_0 = 2406exp^{-0.911q}$
75	-0.1155 (0.2211) $N_0 = 2079exp^{-0.503q}$	-0.0158 (0.8835) $N_0 = 1437exp^{-0.060q}$	-0.1562 (0.0969) $N_0 = 2489exp^{-0.684q}$	-0.0579 (0.6312) $N_0 = 1472exp^{-0.223q}$
100	-0.0777 (0.4068) $N_0 = 1968exp^{-0.421q}$	0.0776 (0.4405) $N_0 = 1199exp^{0.304q}$	-0.1533 (0.1003) $N_0 = 2760exp^{-0.817q}$	-0.1430 (0.2058) $N_0 = 2121exp^{-0.655q}$
125	-0.0204 (0.8246) $N_0 = 1601exp^{-0.121q}$	0.1542 (0.1162) $N_0 = 974exp^{0.681q}$	-0.0913 (0.3235) $N_0 = 2241exp^{-0.537q}$	-0.1557 (0.1548) $N_0 = 2356exp^{-0.720q}$
150	0.0298 (0.7413) $N_0 = 1308exp^{0.181q}$	0.0843 (0.3834) $N_0 = 1176exp^{0.357q}$	-0.0419 (0.6428) $N_0 = 1887exp^{-0.289q}$	-0.1530 (0.1475) $N_0 = 2951exp^{-0.898q}$
175	-0.0356 (0.6932) $N_0 = 1747exp^{-0.221q}$	0.0335 (0.7284) $N_0 = 1331exp^{0.153q}$	-0.0683 (0.4492) $N_0 = 2186exp^{-0.472q}$	-0.1374 (0.1914) $N_0 = 2824exp^{-0.824q}$
200	-0.0493 (0.5851) $N_0 = 1818exp^{-0.286q}$	0.0487 (0.6067) $N_0 = 1283exp^{0.217q}$	-0.0802 (0.3740) $N_0 = 2273exp^{-0.526q}$	-0.1656 (0.1088) $N_0 = 3162exp^{-0.948q}$

Table A-12: Relationships between N_0 and F.

D	CG Lightning	IC Lightning	NBE Lightning
25	0.1092 (0.4753) $N_0 = 1005.2585exp^{0.5810F}$	0.1306 (0.2777) $N_0 = 907.7781exp^{0.5960F}$	-0.0138 (0.9355) $N_0 = 1030.7067exp^{-0.8040F}$
50	0.0059 (0.9602) $N_0 = 1361.0340exp^{0.0340F}$	0.0446 (0.6579) $N_0 = 1237.6875exp^{0.2000F}$	-0.0060 (0.9649) $N_0 = 1189.1571exp^{-0.2960F}$
75	-0.1348 (0.2078) $N_0 = 1956.6713exp^{-0.9260F}$	0.1844 (0.0496) $N_0 = 768.9300exp^{0.9370F}$	-0.1040 (0.3879) $N_0 = 1374.7126exp^{-3.7360F}$
100	-0.1579 (0.1148) $N_0 = 2111.1751exp^{-1.0330F}$	0.1412 (0.1305) $N_0 = 888.0251exp^{0.7540F}$	0.1069 (0.3454) $N_0 = 1115.4353exp^{5.2770F}$
125	-0.0941 (0.3396) $N_0 = 1851.9603exp^{-0.6340F}$	0.0775 (0.4024) $N_0 = 1090.0731exp^{0.4470F}$	0.0713 (0.5166) $N_0 = 1220.4806exp^{3.7160F}$
150	-0.0971 (0.3154) $N_0 = 1861.2433exp^{-0.7100F}$	0.1348 (0.1338) $N_0 = 899.6448exp^{0.7630F}$	0.0261 (0.8062) $N_0 = 1384.3694exp^{1.5950F}$
175	-0.0791 (0.4114) $N_0 = 1793.6358exp^{-0.5610F}$	0.1075 (0.2326) $N_0 = 1011.3082exp^{0.5990F}$	0.0088 (0.9339) $N_0 = 1430.8157exp^{0.5360F}$
200	-0.0201 (0.8323) $N_0 = 1513.2274exp^{-0.1450F}$	0.0913 (0.3115) $N_0 = 1057.8565exp^{0.5390F}$	0.0098 (0.9251) $N_0 = 1450.9880exp^{0.6520F}$

REFERENCES

[1] L. J. Battan. Some factors governing precipitation and lightning from convective clouds. *J. Atmos. Sci.*, 22:79–84, 1965.

[2] A. E. Carte and Kidder R. E. Lightning in relation to precipitation. *J. Atmos. and Tert. Phys.*, 39:139–148, 1977.

[3] T. D. Crum and R. L. Alberty. The WSR-88D and the WSR-88D operational support facility. *Bull. Amer. Meteor. Soc.*, 74:16691687, 1993.

[4] K. L. Cummins, P. E. Krider, and M. D. Malone. The U.S. National Lightning Detection Network^{TM} and applications of cloud-to-ground lightning data by electric power utilities. *IEEE Trans. Electromag. Compatibility*, 40:465–480, 1998.

[5] K. L. Cummins, M. J. Murphy, E. A. Bardo, W. L. Hiscox, R. B. Pyle, and A. E. Pifer. A combined TOA/MDF technology upgrade of the u.s. national lightning detection network. *J. Geophys. Res.*, 103:9035–9044, 1998.

[6] R.J. Doviak and D. S. Zrnić. *Doppler Radar And Weather Observations*. Academic Press, San Diego, CA, 1993.

[7] R. A. Fulton, J. P. Breidenbach, D. A. Miller, and T. O'Bannon. The WSR-88D rainfall algorithm. *Weather and Forecasting*, 13:377–395, 1998.

[8] A. R. Jacobson and M. J. Heavner. Comparison of narrow bipolar events with ordinary lighting as proxies for severe convection. *Mon. Weather Review*, 133:1144–154, 2005.

[9] J. Joss and A. Waldvogel. A method to improve the accuracy of radar-measured amounts of precipitation. *Prepr., Radar Meteorol. Conf., 14th, 1970*, pages 237–238, 1970.

[10] G. D. Kinzer. Cloud-to-ground lighning versus radar reflectivity in oklahoma thunderstorms. *J. Atmos. Sci.*, 31:787–799, 1974.

[11] J. Kuettner. The electrical and meteorological conditions inside thunderclouds. *J. Meteor.*, 7:322–332, 1950.

[12] D. M. Le Vine. Sources of the strongest RF radiation from lightning. *J. Geophys. Res.*, 85:4091–4095, 1980.

[13] T. E. L. Light and A. R. Jacobson. Characteristics of impulsive VHF lightning signals observed by the FORTE satellite. *J. Geophys. Res.*, 107:4756–4764, 2002.

[14] R. E. Lopez, W. D. Otto, R. Ortiz, and R. E. Holle. The lightning characteristics of convective cloud systems in colorado. *Preprints, 16th conf. on severe local storm, American Meteorological Society*, pages 727–731, 1990.

[15] J. S. Marshal and Palmer W. M. The distributions of raindrops with size. *J. Meteor.*, 9:327–332, 1948.

[16] J. S. Marshall, W. Hitschfeld, and K. L. S. Gunn. Advances in radar weather. *Adv. Geophys.*, 2:1–56, 1955.

[17] I. Miller and M. Miller. *John E. Freund's Mathematical Statistics with Applicaions*. Pearson Education Inc., 2004.

[18] R. C. Murty, Israelsson S., E. Pisler, and S. Lundquist. Observations of positive lightning in sweden. *Preprints, Fifth Symp. on Meteorological Observations and Instruments, Toronto, ON, Canada, Amer. Meteor. Soc.*, pages 512–515, 1983.

[19] W. A. Petersen and S. A. Rutledge. On the relationship between cloud-to-ground lightning and convective rainfall. *J. Geophys. Res.*, 103:14,025–14,040, 1998.

[20] M. V. Piepgrass and P. E. Krider. Lightning and surface rainfall during florida thunderstorms. *J. Geophys. Res.*, 87:11,193–11,201, 1982.

[21] J. R. Saylor, C. W. Ulbrich, J. W. Ballentine, and J. L. Lapp. The correlation between lighting and DSD parameters. *IEEE Trans. Geosci. Remote Sensing*, 43:1806–1815, 2005.

[22] Y. Seity, S. Soula, and H. Sauvageot. Lightning and precipitation relationship in coastal thunderstorms. *J. Geophys. Res.*, 106:22,801–22,816, 2001.

[23] X. M. Shao, M. Stanley, A. Regan, J. Harlin, M. Pongratz, and M. Stock. Total lightning observations with the new and improved Los Alamos Sferic Array (LASA). *J. Atmos. Oce. Techno.*, 5:5810, 2006.

[24] S. C. Sheridan, J. F. Griffiths, and R. E. Orville. Warm season cloud-to-ground lightning-precipitation relationships in the south-central united states. *Weather and Forecasting*, 12:449–458, 1997.

[25] D. A. Smith, X. Shao, D. Holden, C. Rhodes, M. Brook, P. Krehbiel, M. Stanley, W. Rison, and R. Thomas. A distinct class of isolated intracloud lightning discharges and their associated radio emmisions. *J. Geophys. Res.*, 104:4189–4212, 1999.

[26] S. Soula and S. Chauzy. Some aspects of the correlation between lightning and rain activites in thunderstorms. *Atmos. Res.*, 56:355–373, 2001.

[27] S. Soula, H. Sauvageot, G. Molinié, F. Mesnard, and S. Chauzy. The cg lightning activity of a storm causing a flash-flood. *Geophys. Res. Lett.*, 25 (8):1181–1184, 1998.

[28] D.M. Suszcynsky and M. J. Heavner. Narrow bipolar events as indicator of thunderstorm convective strength. *Geophys. Res. Lett.*, 30, 2003.

[29] C. W. Ulbrich. Natural variations in the analytical form of the raindrop size distribution. *J. Appl. Meteor.*, 22:1764–1775, 1983.

[30] M. A. Uman. *The Lightning Discharge*. Dover Publications, Inc., Mineola, New York, 1987.

[31] E. R. Willams, S. A. Rutledge, S. G. Geotis, N. Renno, E. Rasmussen, and T. Rickenbach. A radar and electrical study of tropical "hot towers". *J. Atmos. Sci.*, 49:1386–1395, 1991.

[32] W. L. Woodley, A.R. Olson, A. Herndon, and V. Wiggert. Comparison of gage and radar methods of convective rain measurement. *J. Appl. Meteorol.*, 14:909–928, 1975.

[33] Y. Zhou, X. Qie, and S. Soula. A study of the relationship between cloud-to-ground lightning and percipitation in the convective weather system in china. *Ann. Geophys.*, 20:107–113, 2002.